# CONTROL AND OPTIMIZATION OF DIRECTIONAL DRILLING

BY

**MIRZA MOHIBULLA BAIG**

A Thesis Presented to the

DEANSHIP OF GRADUATE STUDIES

**KING FAHD UNIVERSITY OF PETROLEUM & MINERALS**

DHAHRAN, SAUDI ARABIA

In Partial Fulfillment of the

Requirements for the Degree of

## MASTER OF SCIENCE

In

**SYSTEMS AND CONTROL ENGINEERING**

**December 2015**

KING FAHD UNIVERSITY OF PETROLEUM & MINERALS

DHAHRAN- 31261, SAUDI ARABIA

**DEANSHIP OF GRADUATE STUDIES**

This thesis, written by **Mirza Mohibulla Baig** under the direction of his thesis advisor and approved by his thesis committee, has been presented and accepted by the Dean of Graduate Studies, in partial fulfillment of the requirements for the degree of **MASTER OF SCIENCE IN SYSTEMS AND CONTROL ENGINEERING.**

Dr. Moustafa El Shafei
(Advisor)

Dr. Hesham K. Al-Fares
Department Chairman

Dr. Mohammed Faizan Mysorewala
(Member)

Dr. Salam A. Zummo
Dean of Graduate Studies


28th December 2015
Date

Dr. Abdul-Wahid A. Saif
(Member)

Dedicated to My Parents, Sisters and Wife

# ACKNOWLEDGMENTS

All praise is due only to ALLAH subhana wa ta' aala, the sustainer of the worlds, the most merciful for granting me patience, health and knowledge to complete this work.

I would like to thank King Fahd University of Petroleum and Minerals for providing me the opportunity and financial assistance for pursuing MS program.

I would also like to thank National Science, Technology, and Innovation Projects for supporting this project under contract number NSTIP 12-OIL3033-04.

I acknowledge my sincere appreciation and thanks to Dr. Moustafa El Shafei for his supervision and guidance throughout this research. I am grateful to my committee, Dr. Faizan Mysorewala and Dr. Abdul Wahid Al- Saif for their guidance and cooperation.

I appreciate timely assistance from Dr. Mohammed Tariq Nasir and Tri Bagus Susilo in my works.

I would also like to thank all my friends back home and at KFUPM for their encouragement, support and the fun-filled memories shared with them.

I would like to thank my sisters for their love and support during difficult times and to my wife for being there for me.

Last but the most special thanks are for two of the most important people in my life, my parents, for their unconditional love, sacrifices, efforts, prayers and constant encouragement without which I would be nothing and consider myself extremely lucky to have got the best parents in the world.

# TABLE OF CONTENTS

# LIST OF TABLES

# LIST OF FIGURES

# LIST OF ABBREVIATIONS

| | | |
|---|---|---|
| **ROP** | : | Rate of Penetration |
| **ONG** | : | Oil and Natural Gas |
| **DSS** | : | Directional Steering System |
| **RSS** | : | Rotatory Steering System |
| **LQR** | : | Linear Quadratic Regulator |
| **MPC** | : | Model Predictive Control |
| **MWD** | : | Measurement While Drilling |
| **WOB** | : | Weight On Bit |
| **RPM** | : | Revolutions Per Minute |
| **MSE** | : | Mechanical Specific Energy |
| **WPD** | : | Well Pattern Description |
| **BHA** | : | Bore Hole Assembly |
| **DOF** | : | Degree of Freedom |
| **IPO** | : | Interior Point Optimization |

# ABSTRACT

Full Name : **Mirza Mohibulla Baig**

Thesis Title : Control and Optimization of Directional Drilling

Major Field : Systems and Control Engineering

Date of Degree : December 2015

To achieve high well production and improve accessibility of oil reservoirs in complex locations, Directional Steering Systems (DSS) is used for drilling wells in Oil and Natural Gas (ONG) industry. In this work a directional driller consisting of 4 motors is investigated both in its theoretical modeling and control technique.

Currently a basic model is available with the application of Feed Back Linearization in conjunction with LQR for controlling the system. We investigate several directions for improving the model. First investigated approach is for optimization of the system using optimal control technique like Interior Point Optimization. The optimization procedure determines the drilling parameters to minimize the drilling time and the deviation from the planned trajectory. The control is updated at equal distance intervals.

The second approach is to develop a Control techniques, like MPC in order to improve the tracking performance of the model. The control commands include torque of each of the 4 motors. The control is updated at regular time intervals.

MPC and Interior Point Optimization techniques are compared and results are drawn which give an insight about the best methods to be adopted in controlling the system.

# ملخص الرسالة

**الاسم الكامل**: **ميرزا محب الله بيك**

**عنوان الرسالة: التحكم والتحسين من الحفر الموجه**

**التخصص: نظم وهندسة التحكم**

**تاريخ الدرجة العلمية**: ديسمبر 2015

لتحقيق ارتفاع في إنتاج ابار النفط وتحسين إمكانية الوصول إلى مكامن النفط في مواقع معقدة، يتم استخدام نظم التوجيه اتجاهي (DSS) لحفر آبار النفط والغاز الطبيعي(ONG) . في هذا العمل تم دراسة الحفار الذي يتكون من 4 محركات من جوانب النمذجة نظرية ونظم التحكم تقنيه.

حاليا يستخدم النموذج البدائي للحفار مع نظام التحكم الخطي LQR للسيطرة على النظام وتوجيهه. تمت دراسة عدة جوانب وخيارات لتحسين هذا النموذج. بداية تم تطبيق طرق التحكم المثلى مثل التحكم الامثل حول نقطة عمل محددة للنظام. بحيث أن هذه الطريقة تحدد قيم المتغيرات في نظام الحفر من أجل تقليل وقت الحفر و تقليل انحراف جهاز الحفر عن المسار المحدد. وبحيث أن نظام التحكم يحدث تلقائيا بناءا على هذه القيم بعد كل مسافة مقطوعة محددة.

الجانب الآخر من الدراسة هو تطوير نظام تحكم مثل MPC لتحسين تتبع الحفار للمسار المطلوب. بحيث أن إشارات التحكم تحوي على مقدار العزم المطلوب من كل من الاربع محركات للحفار. ويتم تحديث اشارات التحكم بشكل متكرر كل فترة من الزمن.

تمت مقارنة بين طريقة MPC وطريقة التحكم الامثل حول نقطة عمل محددة للنظام وتم عرض النتائج في هذا البحث. وتظهر النتائج الحيثيات التي تبين أفضل طرق التحكم لتستخدم في التوجية والسيطرة على الحفار.

# CHAPTER 1

# INTRODUCTION

## 1.1 General Description

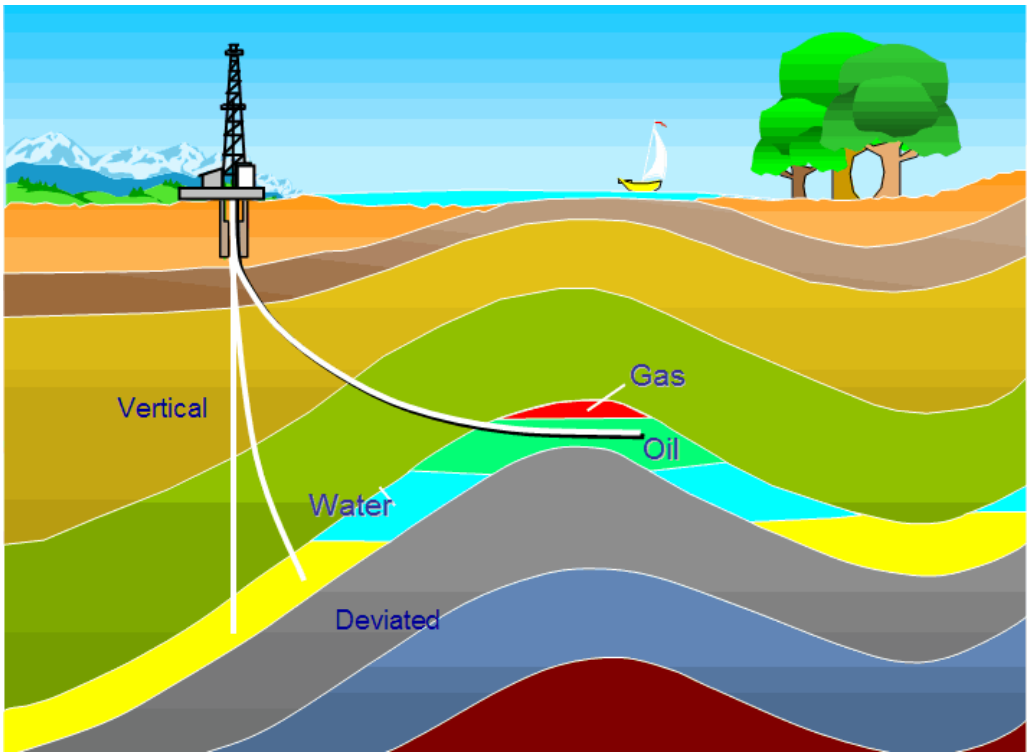


**Figure 1.1: General Schematic (ref: www.rigzone.com)**

Directional Steering System (DSS) plays a significant role in the drilling industry as it achieves high well productivity. It is also effective in complex reservoir locations, and when the oil is distributed in the form of a thin horizontal layer spreading over a large area. Horizontal DSS servers as a means to have a large contact area with the oil reservoir. DSS has substantially reduces the cost of the drilling operations and the total amount of cost.

Thus, there is a lot of focus for the development of DSS mechanisms for drilling and it has become a hot spot for research in the ONG industry.

The major advancement in this area was in 1970's when down hole drilling motors become common. The current state of the art in drilling technology is the Rotary Steerable System (RSS), which provides a controlled DSS having a 3D control of the bit with a continuous rotating drill string, Joshi (1991), Baker (2001), and Eustes (2007).

For an effective directional drilling, the driller must have sufficient knowledge of the position of the drill bit and the direction of the drilling process. A pre-determined path, evaluated by geologist and engineers is given to the directional drillers before the execution of the process. In contradiction to the conventional systems, the DSS require sensors which give a live feed of the position of the system for survey data of the well bore. It provides the estimations of the inclination $\theta$ (pitch angle/ deviation in a vertical direction), the azimuth $\psi$ (deviation from the north of the horizontal plane) and the roll angle $\phi$ (tool face angle) of the drill bit.

**Figure 1.2: A typical Drilling tool (source: www.halliburton.com)**

The directional drilling system includes a drilling assembly, a steering system and a MWD tool. The position sensors which take measurements at regular intervals between 30-500 feet , with 100 feet common during active changes of angle or direction is also a part of MWD. The drilling head assembly consists of a nonmagnetic drill collars, bit, a drill pipe and a high-speed motor. The surveying equipment is encased in the non-magnetic drill collar. After drilling a vertical hole to an appropriate depth then the directional steering procedure begins. The drill head is then placed in the hole. The adjustable housing in the PDM motor is used to direct the drill head towards the desired offset angle. This angle is usually 1.5 degrees to a maximum of 3 degrees. Three- axis magnetometers and three-axis accelerometers are used to determine the azimuth, the inclination and tool face angle. Corrections are regularly made by adjusting rotation speed or the Weight on Bit (WOB).

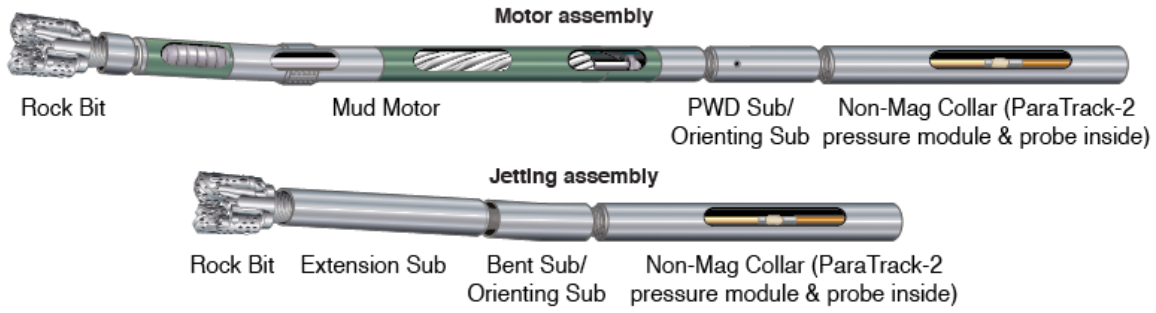


**Figure 1.3: Directional Drilling Tool (source: www.primehorizontal.com)**

During the drilling process the Rate of Penetration ($R_{op}$) is effected by several factors. Bourgoyne et al (1986) proposed an ROP model as a function containing eight multiplied terms. The model consists of several factors like formation strength, formation compaction, and effects of differential pressure, bit diameter, rotary speed, tooth wear and bit hydraulic.

In drilling process, torque and power are considered as the two important controlling parameters. Spanos et al (1995) proposed equations which modeled the torque acting on the drill bit by two terms: former one is related to the dry friction which exist in between the formation and the bit, and the latter one is related to the torque needed to cut the rock. Specific energy theory or log-based rock analysis is used as a standard for bit performance analysis and planning wells.

In this thesis we present a unified approach for the optimization of the drilling parameters and directional steering.

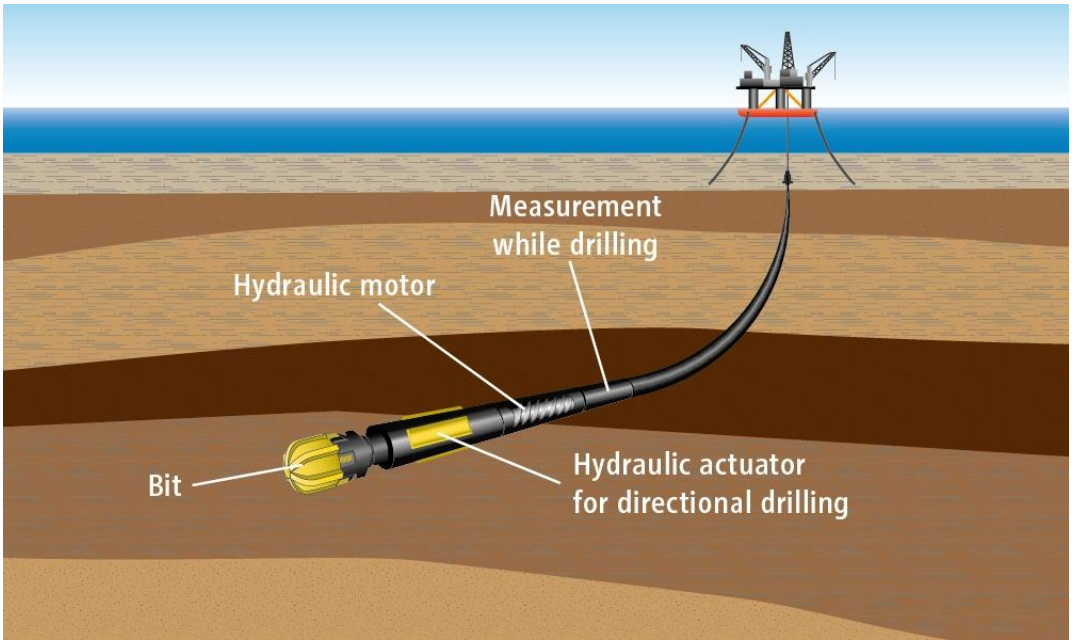


**Figure 1.4: Drilling Assembly (ref: www.rwe.com)**

## 1.2 Problem Formulation

In the model defined by Talib et al (2014), important features such as the influence of rock properties i.e. the rock-bit relations have been neglected. These features should be considered as when we proceed to a practical realization of the system, the above said features play a vital role in determining the performance of the system. For example, during drilling, the type of rock present in the rock bed determines the amount of energy required to crush it. Hard rock like granite requires abundant amount of energy to break and soft rock like sandstone requires less energy. So by varying the torque in an optimal way leads to a reduced amount of energy consumption.

Also, from an industrial point of view emphasis is to be given on the ROP as the efficient increase in ROP will lead to a reduction in time for the drill operation which in turn reduces the cost of the operation in one way. From the literature review, it can be inferred that this

feature is one of the most important one where in ample amount of time and energy have been invested in its research, even this have not been addressed in the previous work. So we will be focusing on the optimization problem using known and feasible techniques.

## 1.3 Objectives

The concept of the system by Talib et al (2014) has shown potential for further research as the proposed design and simulations are still in its early stages. Many assumptions have been considered in the model which needs to be taken into account in order to refine it and take it a step towards its industrial realization.

So the goal of this thesis can be summarized into 4 points.

1. Apply an optimization technique to reduce the deviation in the trajectory tracking and optimization of drilling parameters for reducing time and thereby increasing the ROP of the system.

2. Study the effect of rock formation using the data on rock formation for simulating the system.

3. Application of an additional control technique to improve tracking.

4. Compare the performance of the two approach.

## 1.4 Approach

In our work we will first address issues in our developed model.

1. The varying rock specific energy is used as a tool to add disturbance to the model. We will create a land profile using field data in order to vary the rock specific energy. Work by could be used to gather the specific energy data for different types of rocks beds and create a land profile.
2. Application of Optimization algorithm using interior point algorithm to optimize ROP
3. Application of MPC to the system to improve tracking
4. Comparison in the two approaches
5. Results and Conclusion
6. Future Work

## 1.5 Thesis Organization

The organization of this thesis is as follows. Chapter 2 presents a literature review. The modeling of DSS is covered in chapter 3. In chapter 4, the interior point algorithm optimization is presented In Chapter 5, the MPC control design is presented and the proposed controller is evaluated by tracking the desired trajectory and Chapter 6 concludes the thesis work and presents a few future extensions.

# CHAPTER 2

# LITERATURE REVIEW

Before we look deep into the recent trends in the optimization work in DSS, it is necessary to review some of the technical aspects of the Drilling system.

## 2.1 Factors effecting DSS Performance

Several factors such as mud composition, hydraulics, rock characteristics, wellbore pressure, bit design and condition, and bit operating parameters are the factors that has an influence on the DSS performance.

### 2.1.1 Rock Characteristic's

Rate of Penetration (RoP) is affected by the formation strength of the rock and elastic limit. However, ROP can be changed by the mineral composition. For example, rocks having a high composition of abrasive materials will cause the bit teeth dulling while those have higher volumes of clay will cause the ball up of bits.

### 2.1.2 Wellbore Pressure and Bottom-Hole Confining

Effective confining stress is the difference between pore pressure and the wellbore pressure. This has a direct effect on the rock strength. An increase in confine strength will result in an increase in both strain and stress to fail the rock. And, this increase will result in an increase in effort required to fail the rock. So, as the effective confine stress increases ROP decreases.

### 2.1.3 Bit Design

Bit design includes the bit shape, tooth length, size, angle of cutters, nozzle and jet design etc. These characteristics influence the bit performance and the ROP of the system. Bit condition, such as bit wear effects the performance of drilling and an increase in wear thereby reduces ROP and bit performance.

### 2.1.4 Mud Composition

ROP is also effected by the drill fluid properties. Some of the properties having influence on bit performance are flow properties, size distribution and solid content, chemical composition and density.

### 2.1.5 Bit Operating Parameters

**Weight on bit (WOB): 'It is the amount of the axial force applied to the bottom-hole formation to break the rock by the bit.'** The difference in drill string weight during the operation and during the off-bottom rotation is the way to calculate WOB. A typical plot of WOB vs ROP, with constant drill parameters is as shown in Figure **2.1**. It can be conferred from the plot that a significant ROP can be obtained only after reaching the threshold WOB. Then the penetration rate rapidly increases with increasing WOB , and at a higher value the increase in ROP is small. Finally at an extreme high value of WOB, ROP no longer increases. This point is called bit floundering and flounder point is the point at maximum ROP.

In case of shale, an increase in WOB after the flounder point leads to a decrease in the Rop. As depicted in Figure 2.2, after crossing the flounder point , the bit starts to ball up and become ineffective and thereby reducing the ROP of the system and there is no way of reaching the previous high peak in ROP as well.

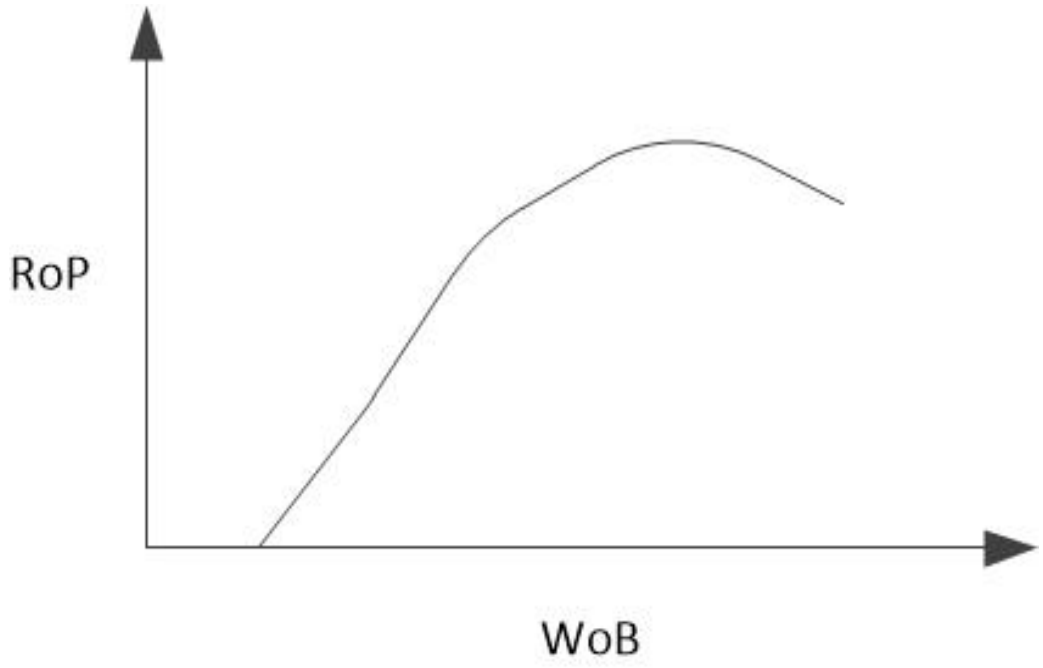


**Figure 2.1: ROP vs. WOB (normal Condition)**

**Rotary Speed:** Under normal circumstances with all other parameters held constant, the ROP increases with low RPM values. As the RPM increases, the rate of increase in RPM reduces. This poor response to RPM, is due to poor bottom hole cleaning at high RPM. It is a good drill practice to choose an appropriate combination of WOB and RPM for different rock types. For example, high strength rock needs to be drilled with low rpm and high WOB and vice versa for low strength rock bed. Also, there is a chance for stick slip at low RPMs, therefore the preferred RPM is moderate.

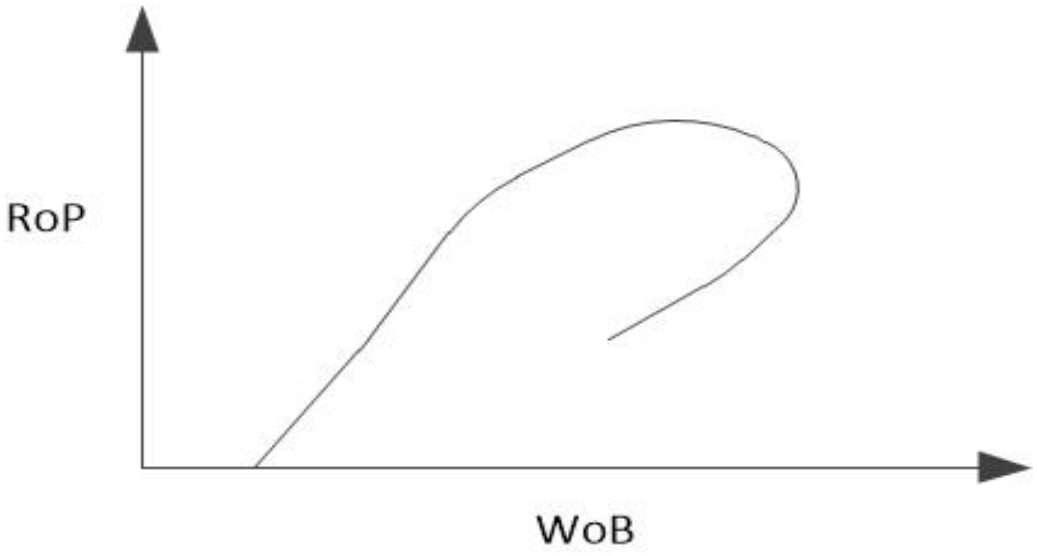


**Figure 2.2: ROP vs. WOB (Balling)**

**Hydraulics: ROP** is also influenced by flow rate of drill fluid and the bit hydraulics. The flounder point is also affected by the level of hydraulics. An increase level of hydraulics will result in an increase in the flounder point hence achieving higher levels of Rop. These flounder points are formed when the cuttings are not removed as quickly as they are generated.

## 2.2 Relationship between Surface Data and Bottom-Hole Data

### 2.2.1 WOB, Torque, and RPM

Calibration of WOB is done at the start of the drill operation where it is set as zero and origin is set at the hook load. During drilling, the difference in the original hook load and the actual hook load defines the WOB. Measurement of Torque is through the load current given to the drive and measurement of RPM is done by sensors at the rotary table.

### 2.2.2 Rate of Penetration (ROP)

The conventional method of measuring the ROP is through the measurement of the downward motion of the drill string upper end via a drill line travel or measuring block.

However, due to the elastic nature of the drill string, there is a range of errors occurring in the measurements due to physical deformities during the drill process. So, in order to minimize the error in the estimate, the ROP is usually determined by the average value of drill rate over a period of time or dept.

## 2.3 Research Trend in the area of Directional Drilling

In parallel to the development of the BHA, an important factor which was under constant research was the way to increase the efficiency of the system viz-a-viz increase in ROP to reduce cost of drilling. Arranged chronologically are the works on drilling optimization.

In the first half of the 90's era, Fear et al (1992) used a risk analysis approach to formulate a bit-run cost optimization method, in which they incorporate the interdependence of drilling events and bearing life. The technique also provided a formal method for assessing the opportunity cost for using a device to detect bit-bearing failures down hole.

In the research done by Belaskle et al (1993) the main focus of the work was on enhancement of measuring while drilling (MWD) techniques which can in-turn help in optimizing roller cone bit runs and polycrystalline-diamond-compact (POC), planning high-departure wells, improving predictability, performance and minimizing surface torques . During the same time Aarrestad and Balikra (1994) worked on the various torque

and drag problems encountered during drilling wells. They also discusses on the use of torque and drag calculations in planning of drilling operations with optimal torque and drag effect and hole cleaning in long reach well profiles.

While the second half of the 90's Imrich et al (1996) provided research on the utilization of simple fuzzy expert diagnostic system for evaluation of diamond core drilling by means of impregnated diamond bits. For this purpose the knowledge base consisting of precise data of monitoring of drilling and experiences of drilling experts was created and utilized.

Also another benchmark research was done by Karu (2005) in which a new model was used to revisit classical theory of hydraulic optimization. The new methodology was used to determine the optimum gas/liquid injection rates for maximizing drilling rates while using foam in vertical wells by keeping a low downhole pressure. This method was used to determine the best combination of gas/liquid injection rates and total bit flow area (nozzle size) to maximize drilling rate.

As the research flourished, a new interest in Directional drilling took place by Warren (2005) who claimed that Casing while drilling (CWD) which is dominant in vertical drilling in reducing drill cost and solving drilling problems could be applied to directional drilling as well. They concluded that CwD works efficiently with similar advantages for directional drilling as it did for vertical ones and removes the effort of re-running a casing after drilling which was prevalent in previous times.

In a parallel research, Osterloh and Menard (2007) dealt with a broader perspective of optimization which focused on the decision of placement of horizontal wells. This paper deals with two new methods to optimize the output of a gigantic geologically complex oil

field. Usually for very large oil field the Decision and Risk analysis procedure will take years due to large number of expansion and development scenarios for analysis. First is a semi-automated spreadsheet which quickly select and places thousands of hypothetical horizontal well in a multi-million grid block model. Second, is a multivariate nonlinear interpolation method that enables a full field forecast calculations in seconds, as compared to long durations of approx. 20 hours by using traditional simulations. It concludes by stating that the described simulation tools assisted in an optimal decision analysis to solve complex problems can be completed in a matter of days in comparison to the traditional methods.

Another innovative approach was taken by Rashidi et al. (2008), wherein they proposed a method to determine real time bit wear. This method was based on combining Rate of Penetration (Rop) model and Mechanical Specific Energy (MSE) Model. An extensive study was shown to demonstrate the effect of varying bit designs, bit wear and drilling parameters on Rop. With the use of ROP models it was determined that an optimum bit design and type with related drilling parameters could be globally recommended for an entire bit run.

Adding to the diversity of research for optimization, an interesting papers was published by Dhal (2008) focuses on the importance of removing drill solid from drill liquid with the use of shaker screens so optimization of filtration efficiency and screen life is discussed. The paper proposes different configuration of shaker screen and scree cloth in order to reduce screen wear by 90% and increase the segregation of solid and liquid waste by 95%. This paper mainly focuses on double deck shakers. It concludes by explaining how the double deck shaker should be operated to minimize wear on the primary screen and how

the solid removal from drilling fluids is optimized which in turn reduces the cost of drilling operation.

At the end of the first decade of 21st century, a few benchmark works took place. The first one by Motahhari et al (2009) was directly related with our research question.

During a drilling process, for manipulating the drill trajectory, the drill string temporarily stops rotating till the bent housing the PDM (positive displacement motor) is oriented in the desired direction and in turn this effects the ROP. Hence, there is a need to optimize BHA operation with the optimization of PDC drill bits. The authors discusses how ROP model coupled with motor performance data can be used to predict the optimal WOB for achieving in maximum ROP for a required area of hole to be drilled. By using this approach we can solve the ROP model and predict the ideal Weight on Bit in lieu of the restrictions imposed by the PDM performance equations. The analysis is done in optimizing a section of well bore which takes into consideration the wear on the Bit. Two different types of formations are used to test the optimization procedure along with a field test using two different types of motors. The outputs of the analysis are the differential pressure values, maximum average ROP and the Weight on Bit. This approach can be used to achieve a better combination of PDC/PDM bit for achieving a good Rate of Penetration over a vast range of operating conditions. So, in conclusion, the procedure discussed in the paper is used to estimate an optimum Weight on Bit for a given section of drill operation.

Some of the additional applications could be that the drill interval can be divided into much smaller intervals and an optimum WOB could be estimated for each of them so that there will be an overall increase in the ROP of the system. This method could be easily used by any bit design, bit type and ROP model.

Secondly, in the paper by Karkoub (2009) the technique of preventing the breaking of drill string by suppressing torsional vibrations (stick-slip oscillations) using PID and Lead-Lag controllers in conjunction with genetic algorithms is discussed. Simulation results are presented to validate the scheme. It was noted that these vibrations decrease the ROP and increase the cost of well and can interfere with MwD and induce well instability.

And lastly, an extensive research was done on optimization by Judzis et al (2009) where in a full scale Lab test in conjunction with field test were performed for drilling in over 10000 psi pressure with 4 different drill bits 6inch, 3 types of rocks and 5 different drilling fluids.

They concluded by highlighting the following points

- Lab data was at par with the field data
- ROP reduced by mudding up at high bottom hole pressure
- Relationship btw ROP and rock strength is not a simple function of bottom hole pressure
- MSE at high bottom hole pressure is higher than rocks compressive strength, even when the drill bit is drilling efficiently

A model was developed by Tuna and Evren (2010) which optimizes the drilling parameters such as bit rotation speed, weight on bit (WOB) during the drilling operation to minimize the overall drilling cost, cost per foot and maximize Rop. Actual field data obtained via data recording systems and modern well monitoring systems was used by the developed model to predict the rate of drilling as a function of the drilling parameters. As per the study ROP of drilling could be predicted with high accuracy on the basis of the previous drill

trend. To achieve minimum drill cost, the optimum bit rotation and WOB could be determined.

And during the last few years an innovative technique was developed by Onwunalu (2011) approached the optimization problem by optimizing well placement in large scale field developments involving many wells. A new algorithm called well pattern optimization (WPO) consisting of well pattern description (WPD) is used in optimization.

In the WPD, each solution consist of a representation of well pattern along with pattern operators that alter the shape, size and orientation of the pattern. Multiple pattern is considered in WPD. It is the parameters associated with the WPD which are determined in optimizations. These optimizations are used in increasing the Net Present Value of the wells. A case study of 4 wells was done to validate results.

A description of an autonomous drilling system was developed and field tested by Koederitz and Johnson (2011). The drill performance was evaluated by the use of a test process run by the system software on a set of target points. A research method was used in identifying these points which was based on an early work in the application of real time Mechanical Specific Energy display. It was concluded that the results from the field test had the potential for an autonomous drilling optimization without the drilling knowledge and the procedure was economical, practical and flexible in many cost effective applications.

Contreras (2012) presented work in estimating the pore pressure in a sub pressure basin. Pore pressure is calculated using sonic logs and modified D exponent by use of Eaton's method (Eaton 1995), and the optimization method was carried out using apparent-rock-

strength log (ARSL) and by using different bits and operational parameters in different sections of the well.

The test results of various simulations are compared and the best combination is selected by calculating ARSL. All these calculations are done by a dedicated software.

Fu and Li (2012) introduced a new tool called hydraulic pulse cavitating jet generator to improve the ROP of the driller. When the drilling fluid enters through the tool, it is pulse modulated and cavitated (addition of vapor cavities) which creates a pulsed cavitating jet at the outlet of the nozzle. Because of this the cleaning efficiency of the well bottom cuttings is increased and the ROP is improved. A large number of field test and lab test conformed an effective boost in ROP.

Interestingly, a separate work on attitude control was presented by Panchal et al (2012) where in the attitude is represented by a unit vector, thus the non-linearities introduced by Euler angle representations are avoided. Three control laws are proposed, and their stability is proven. Their behavior is tested by numerical simulation. The merits of the laws from an engineering perspective are highlighted, and some details for the implementation of the laws on directional drilling tools are provided.

In the end, yet 4 types of work have caught the attention of researchers interested in our research question. The first one is by Park et al (2013) in which the author states that “As the importance of unconventional resource grows, the demand for the directional drilling technology is increasing”. In his work, he proposed a new RSS deploying hybrid 4-pad system. In this mechanism, by taking advantage of both ‘point-the-bit’ and ‘push-the-bit’ types, steering angle is improved.

And secondly, Sui et al (2013) talks about real time optimization of ROP during drilling operation. In this paper, the effects of several parameters while drilling was studied by using the Young's ROP model. An advanced method for optimization and calculation of ROP was presented. The method was called moving-horizon multiple regression, which worked on the technique if continuous calibration of ROP model coefficients using the real time data and thereby reducing the estimation error of the existing models. Also, an MPC strategy was used for achieving the ROP optimization and satisfy drilling requirements. The data used in their demonstration was from the North Sea well.

Geological information can be actively obtained during drilling by using Logging While Drilling (LWD) and Seismic While Drilling (SWD) tools placed at the BHA. Yan Chen et al (2015) utilized these tools to show an automated workflow for proactive geo-steering through continuous updating of the estimates of the earth model and robust optimization of remaining well path under uncertainty. The use of these tool to obtain real time geological data lead to improved recovery during drilling.

An interesting issue in the current drill system was investigated by Marck and Detournay (2015). The influence of RSS design on borehole spiraling was studied and in particular the push-the-bit type was selected. With their study, they concluded that the actuation mechanism for the push-the-bit pads influence the directional stability of the system.

# CHAPTER 3

# MODELING OF DRILLING SYSTEM

The current drill technology used in directional drilling is the RSS or the Rotary Steerable System as shown in Figure 3.1. Directional Drillers or the MWD engineers are the ones who generally program the system and steer it using surface equipment to which the tool responds and moves in the commanded direction. In short, it is a tool which is designed to directionally drill with a continuous rotation from the surface.

This technique of directing the well path can be broadly classified into two categories, these being the point-the-bit and push-the-bit. The former work on the method of bending the main shaft running along the tool towards the desired direction of motion and requires some form of a non-rotating housing for creating such a deflection. While the latter make use of pads which presses on the well bore thereby causing the drill bits to press in the opposite direction resulting in the change of the drilling path.

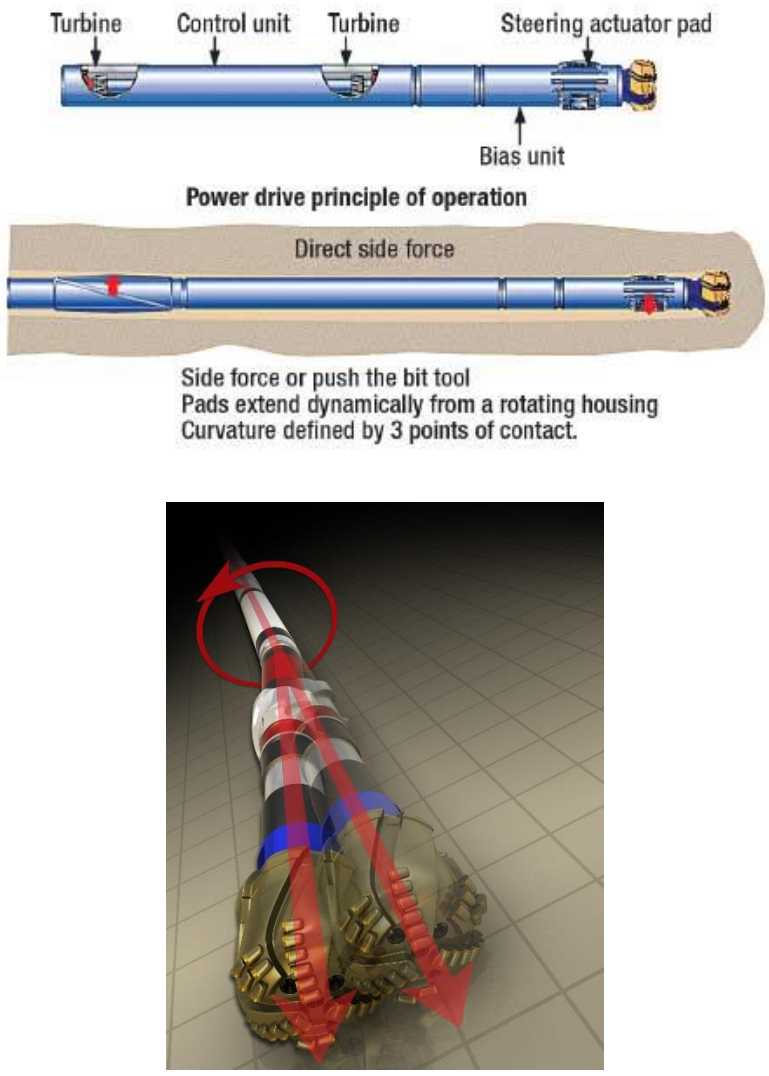


**Figure 3.1: Cross Section schematic and Physical Structure of Single motor RSS (www.gyrodata.com)**

## 3.1 Quad Motor BHA Description

Till now many concepts have been proposed for the type of BHA to be used for drilling of which the most predominant type is of a Single motor system with variations in Drill bit shapes to provide optimum results. These are the ones which are being used in the market today.

Recently a new model was proposed by Talib et al (2014) consisting of four motors controlling four drill bits in a BHA. The model was designed and simulated by considering a few assumptions. The details of the model is as follows.

### 3.1.1 Mechanical Representation

The experimental Directional Steering System (DSS) is equipped with four motors (5) as shown in **Figure 3.2** having a drill bit attached to each of them. These motors are independent from each other for their control giving the user the freedom to manipulate their speed for a precise control on the rate of rock removal and the direction of movement of the drill head. This assembly is attached at the end of the drill string (2) which is responsible for carrying the drilling fluid from the surface to the area of drilling operation. A precise control of the direction of drilling and the optimization of ROP can be achieved by the use of four motors in conjunction with the traditional drilling variables. The direction of rotation is clockwise for the top and bottom motors while it is anti-clockwise for the left and right motors. Pitch action is obtained by decreasing/increasing the speed of the top motor while increasing/decreasing the speed of the bottom motor. The azimuth is obtained likewise using the left and right motors. A fine management of the drilling process under varied operating constrains and under various drill environment is obtained by the control of the four motors.

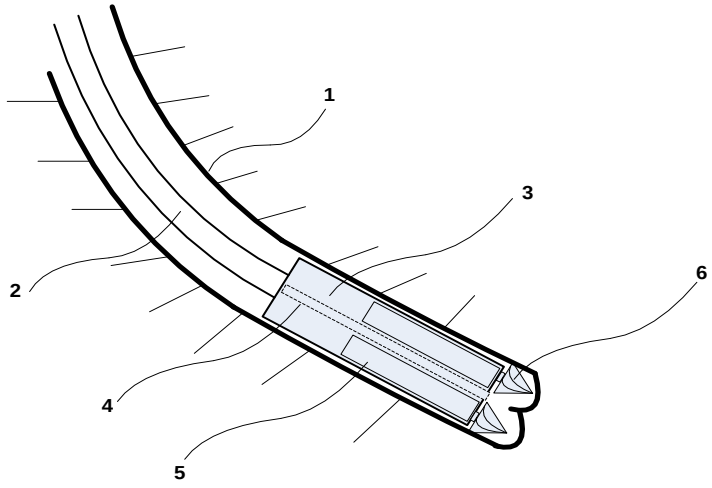


**Figure 3.2: Overview of the drilling assembly**

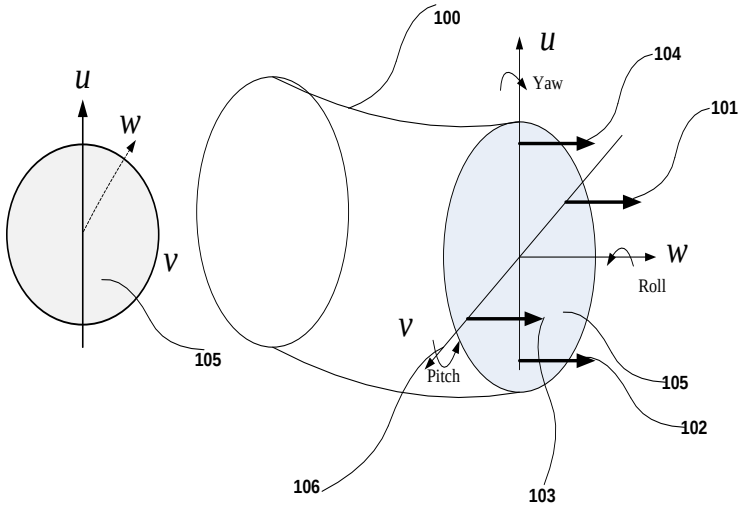


**Figure 3.3: Reference axis for the drilling assembly**

According to one embodiment, shown in Figure 3.3, Bore hole is (100). There is a symmetric arrangement of the drill bits w.r.t {u, v, w} (the body axes) (106), where the axis w depicts the direction of motion in perpendicular to the page. {u, v} plane is taken as the tool face (105). (101) is the left motor thrust, (102) is the bottom motor thrust while (103) and (104) are the right and top motor thrust respectively. There is a clock-wise

direction of rotation for rotors (103) and (104) while (101) and (102) are rotating counter clock-wise. The mud motors can be hydraulic or electric with rpm/torque sensors and power control. The pitch, yaw and roll direction is also depicted in the Figure 3.3

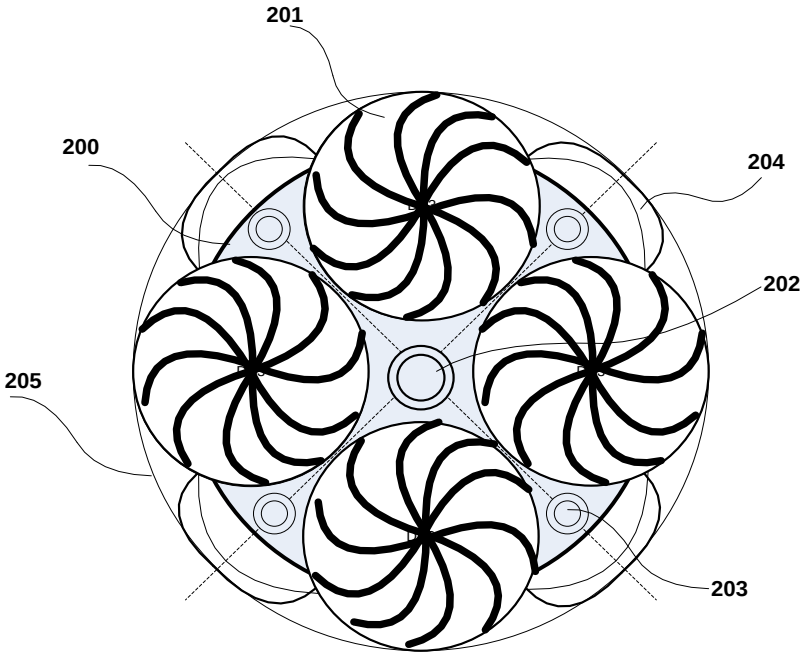


**Figure 3.4: The drilling assemble front projection**

Figure **3.4**, depicts the schematic of the BHA as projected towards the tool face. (200) is the BHA cylindrical casing, and (205) is the bore hall. (202) is the central nozzle for ejecting the drilling fluid (mud), (203) are four side nozzles for removal of circumferential rock chips, (204) front chisels fixed to the drill body for crushing circumferential debris and smoothing the surface of the borehole. (201) are four conic drill bits with twisted blades for crushing and removal of the rocks.

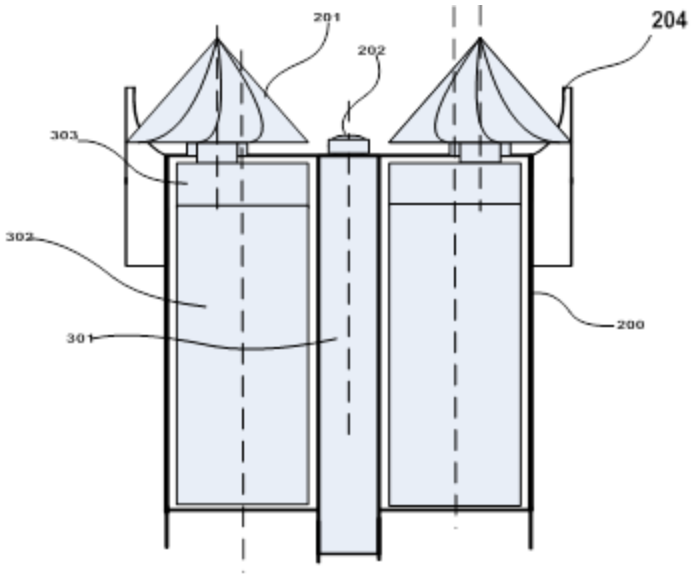


**Figure 3.5: Side cross section of the drilling assembly**

Figure **3.5** depicts a longitudinal cross section view of the drilling head assembly showing two motors (out of four) (302). A body (200), the central nozzle (202), a central pipe (301) for carrying the inlet mud fluid. The figure also shows two drill bits (out of four) (201) connected to the motors via a gear box (303). The chisels (204) help to crush rocks and smooth out the circumference of the bore hole. The drilling fluid can be made to be in contact with motors heat sinks to cool the motors.

The BHA, Figure 3.6, may include a section for conventional Measurements while drilling MWD (504), and another section for conventional log while drilling (LWD) (505), in addition to other instruments for measurement of body angular velocities and acceleration to track the orientation and position of the BHA. The MWD includes three perpendicular set of accelerometers for gravity measurements to determine the vertical axis, and three magnetometers for determining the magnetic north. The accelerometers and

magnetometers are aligned with the BHA body axis, The BHA may also include a hydraulic generator and other motor control electronics and actuators.

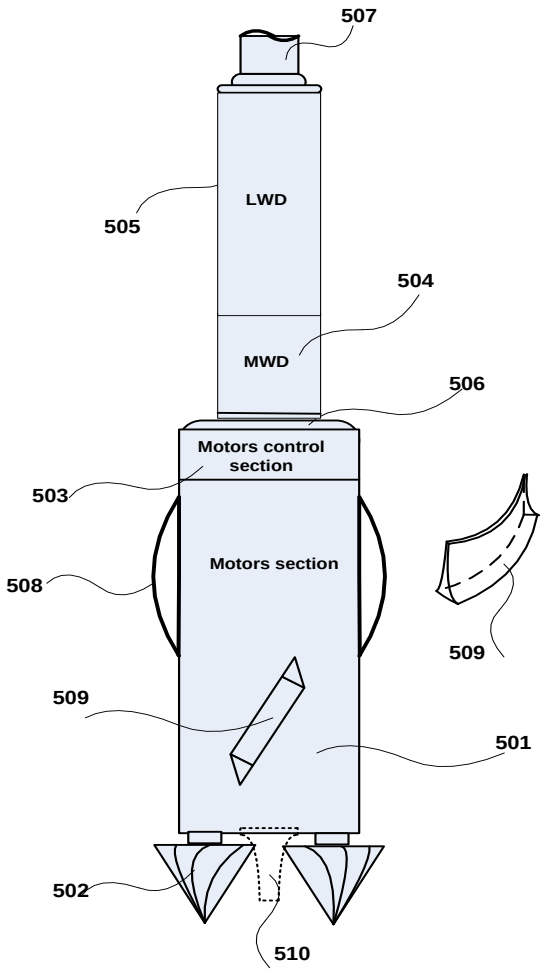


**Figure 3.6: Components of the BHA**

Attached outside the drilling head plurality of sliding surfaces (508) along the longitudinal axis to reduce friction during horizontal drilling. The sliding surfaces could be housed inside the drilling head casing and brought out when needed. Attached out also outside the surface of the drilling head a plurality of smoothing surfaces (509) inclined to the longitudinal axis to smooth the borehole. Similarly, front chisels are also attached to

drilling head to remove left over rock parts, which could be inaccessible by the four drilling bits.

**Table 3.1: Comparison of Single motor and Quad motor RSS**

| **RSS Single Motor** | **RSS Quad Motor** |
|---|---|
| Only 4 manipulated variables i.e. 1 RPM,1 Torque, Fluid Pressure and WOB | Have 9 manipulated variables i.e. 4 RPM, 4 torque and WOB |
| Comparatively difficult to maneuver | Easy to maneuver |
| Takes time to shift position i.e. the system halts and then the drill head inclines towards the desired direction and then drilling is resumed | No need of such halts for changing the direction. Drilling action is continuous. |
| Drill string is rotating | No need for drill string rotation |
| Torsional vibrations are high | Very Low vibrations in drill string due to lack of drill string rotation. |

### 3.1.2 Mathematical Representation

The drill bit resolves the torque of the motor into two components; a lift force ($F_{Li}$) and a drag torque which is perpendicular to the bit axis ($T_{\mathrm{Di}}$). The following mathematical modeling assumes the four down hole motors are DC motors. However, the mathematical model is also valid for hydraulic motors and other motor types with minor changes.

The equation of the motors is given by

$$T_i = \frac{K_t}{R_m}[E_{si} - K_m\omega_i], \qquad i = 1,2,3,4 \tag{1}$$

where, $T_i$ is the torque of the i[th] motor, $\omega_i$ is the speed of the i[th] motor, $K_t, K_m$ are motor torque constants, $R_m$ is the motor electrical resistance, and $E_{si}$ is the motor supply voltage.

Depending on the nature of the rock, a minimum amount of energy is required to crush the rock. Rock Specific Energy, $E_{rs}$ in J/m$^3$, is defined as the energy required to crush a unit volume of the rock.

From the energy balance equations, equating the mechanical power by the four motors to the rate of rock crushing, we get

$$\sum_{i=1}^{4} T_i\omega_i + W_{ob}\dot{w}_b = \dot{w}_b A_h E_{rs} \tag{2}$$

where $\dot{w}_b$ is the rate of advance of the drilling head in m/sec, also known as the rate of penetration ($R_{op}$), and $W_{ob}$ is the weight on bit. Finally, $A_h = \frac{\pi D_h^2}{4}$ is the cross sectional area of well bore, and $D_h$ is hole diameter. The $R_{op}$ is given by

$$R_{op} = \dot{w}_b = \frac{\bar{\Delta}\bar{\omega}}{2\pi} \tag{3}$$

where $\bar{\Delta}$ is the average penetration rate of the 4 bits per revolution, and $\bar{\omega}$ is the average angular velocity of the four motors. $\bar{\Delta}(t)$ is function of many factors including the rock specific energy, hole Wob, the total motor torques, bit geometry, and drilling fluid. However, it can be adjusted using Wob as shown in the following approximate equation

$$\overline{\Delta}(t) = \left( \frac{2\pi \sum_{i=1}^{4} T_i}{A_h Ers - Wob} \right) \tag{4}$$

$$\overline{\omega} = (\omega_1 + \omega_2 + \omega_3 + \omega_4)/4 \tag{5}$$

The lift force of bit consists basically of two components. The first one $F_{Li}^{a}$ which move the drilling debris up through the drill flute, and may be approximated by

$$F_{Li}^{a} = \frac{1}{2} A_{bi} \beta_{bi} D_{bi} \rho_r \dot{w}_{bi}^2 \tag{6}$$

Where $A_{\text{bi}}$ is the cross section are of the i$^{\text{th}}$ bit, $\beta_{\text{bi}}$ is a parameter which depends on the bit structure, $\rho_r$ is the rock density, $\dot{w}_{bi}$ is the rate of penetration of the bit.

The motor work in crushing the rocks is substantially greater than the motor work to remove the debris. As such the $F_{Li}^{a}$ will be neglected. The bit drag torque, the torque used for crushing the rocks, $T_D$ can be approximated by

$$T_{D_i} \approx T_i \tag{7}$$

This approximation is justified because the work done by the motor to crush the rocks is substantially bigger than the work to move the debris.

The second lift force $F_{Li}^{b}$, is the equivalent thrust force that causes the BHA to move forward. The power used by the drag torque is equivalent to the thrust force time the rate of penetration that is

$$T_{Di} \omega_i = F_{Li} \dot{w}_i \tag{8}$$

But

$$\dot{w}_i = \frac{\Delta_i \omega_i}{2\pi} \tag{9}$$

Hence, for $i$=1, 2, 3, 4

$$F_{Li} = (\frac{2\pi}{\Delta_i}) T_{Di} \tag{10}$$

Where, $\Delta_i$ is the feed rate per revolution and $T_i$ is motor torque.

$F_{L1}$ and $F_{L3}$ are lift forces of the top and bottom rotors, while $F_{L2}$ and $F_{L4}$ are the lift forces of right and left motors.

$\bar{\Delta}$ can be inferred online using Eq.(4) from the measured $R_{op}$ and the measured angular velocities of the motors. The forces and torques acting on the Bottom Hole Assembly (BHA) can be better described by the following auxiliary inputs:

$$u_1 = F_{L_1} + F_{L_2} + F_{L_3} + F_{L_4} \tag{11}$$

$$u_2 = F_{L_2} - F_{L_4} \tag{12}$$

$$u_3 = F_{L_1} - F_{L_3} \tag{13}$$

$$u_4 = T_{D_1} + T_{D_3} - T_{D_2} - T_{D_4} \tag{14}$$

$u_1$ is related to the total thrust of the four motors. Due to the close proximity of the positions of the 4 drill bits, the force exerted by each drill bit could be summed up into a total thrust.

While, $u_2$ generates moment responsible for changing the azimuth direction. A difference in force exerted by the two drill bits located on the horizontal plane of the BHA leads to a Yaw motion in the drill action. An increased force applied by the bit (103) will make the driller move in the left direction while an increase in the force by the bit (101) will make it tilt towards the right.

Similarly, $u_3$ generates the moment for changing the inclination. A difference in force exerted by the two drill bits located on the vertical plane of the BHA leads to a pitch motion in the drill action. An increased force applied by the bit (104) will make the driller move in the downward direction while an increase in the force by the bit (102) will make it tilt towards the upward direction.

While $u_4$ generates the torque for the roll motion. Since the motors on the adjacent side are rotating in one direction i.e. (101) and (102) are rotating CCW and (103) and (104) are rotating CW, the difference in the torques generated by the opposite motors describe the roll action of the assembly.

Describing vectors not only in inertia frame, but also in a body frame is convenient when dealing with drilling objects. The center of the inertial frame is assumed to be the control room location on the oil rig. This is called the earth frame. The inertial frame is defined by $\{X_E, Y_E, Z_E\}$, where $X_E$ points to the geographic north, and $Z_E$ points to the earth center. The body attitude is described with respect to three virtual body axis, $\{X_B, Y_B, Z_B\}$ located at the body reference point $O_b$. These three reference axis are assumed to be parallel to the inertia axis.

When a vector is seen with respect to the earth fixed frame it will be denoted with a $E$ subscript. Likewise if the vector is seen with respect to the body frame will be subscripted with $B$ or b. The BHA position in terms of the inertial frame is represented as the vector in equation (15)

$$\zeta^T = [x_E, y_E, z_E]. \tag{15}$$

The orientation of the BHA will be described by the rotation of the body fixed frame {$U_B$, $V_B$, WB}, with respect to {$X_B$, $Y_B$, $Z_B$}.

The orientation of the drilling assembly is represented by the three Euler angles, namely the roll angle $\phi$, the Pitch angle $\theta$, and , the yaw angle $\psi$, and presented in the vector

$$\Omega^T = [\phi, \theta, \psi]. \tag{16}$$

Initially it is assumed that the body axis {$U_B$,$V_B$,$W_B$} is aligned to {$X_B$,$Y_B$, $Z_B$}.

The orientation matrix can be described the rotational matrix $R_{BE}$ given by

$$R_{BE} = \begin{bmatrix} c\psi c\theta c\phi - s\psi s\phi & -c\psi c\theta s\psi - s\psi c\phi & c\psi s\theta \\ s\psi c\theta c\phi + c\psi s\phi & -s\psi c\theta s\phi + c\psi c\phi & s\psi s\theta \\ -s\theta c\phi & s\theta s\phi & c\theta \end{bmatrix} \tag{17}$$

The rotational matrix $R_{BE}$ defines the body to inertial axes transformation, for a point $P$ in space, where $s\theta$ denotes $sin\,\theta$ and $c\theta$ denotes $\cos\theta$ .

$$P_{XYZ} = R_{BE} P_{UVW} \tag{18}$$

The inverse transformation matrix $Q$ is given by

$$Q = R_{BE}^{-1} = R_{BE}^T \tag{19}$$

$$R_{BE}^T = \begin{bmatrix} c\psi c\theta c\phi - s\psi s\phi & s\psi c\theta c\phi + c\psi s\phi & -s\theta c\phi \\ -c\psi c\theta s\psi - s\psi c\phi & -s\psi c\theta s\phi + c\psi c\phi & s\theta s\phi \\ c\psi s\theta & s\psi s\theta & c\theta \end{bmatrix} \tag{20}$$

$$P_{UVW} = Q P_{XYZ} \tag{21}$$

The direction of gravitational force is down to the earth fixed frame.

$$\begin{bmatrix} g_x \\ g_y \\ g_z \end{bmatrix} = Q \begin{bmatrix} 0 \\ 0 \\ g \end{bmatrix} = \begin{bmatrix} -s\theta c\phi \\ s\theta s\phi \\ c\theta \end{bmatrix}. \quad (22)$$

The gravitational force components on the body in $U_B$& $V_B$ directions are

$$f_{gu} = -s\theta c\phi mg \quad (23)$$

$$f_{gv} = s\theta s\phi mg \quad (24)$$

These two components are cancelled by formation reaction forces as the motion of the drilling assembly is confined to the bore hole and no lateral motion is possible. But, these two components determine the friction torque against angular motion and the friction forces in the direction of motion around $w$-axis as shown in equation (25) and (26)

$$F_f = \mu_1 * (s\theta c\phi mg + s\theta s\phi mg) * \dot{w}_b \quad (25)$$

The frictional force is max during horizontal drilling i.e. (at $\theta = 90$) and during vertical drilling it is negligible. Similarly, the frictional torque can be written as

$$T_{fw} = K_w \dot{\phi} \quad (26)$$

The total sum for torques $T_{ext}$ acting on the BHA can be described as:

$$T_{ext} = T - T_G - T_f \quad (27)$$

By Newton's law, the BHA attitude dynamic equation is given by

$$T_{ext} = J\dot{\Omega} + \Omega \times (J\Omega) \quad (28)$$

On substitution of the equation 28 in equation 27 we get

$$J\dot{\Omega} + \Omega \times (J\Omega) = \begin{bmatrix} L_b u_2 \\ L_b u_3 \\ L_b u_4 \end{bmatrix} - T_G - T_f \tag{29}$$

Where, $I_r$ is inertia of the motor/drill bit and $J$ is the BHA moment of inertia matrix

$$J = \begin{bmatrix} I_{xx} & 0 & 0 \\ 0 & I_{yy} & 0 \\ 0 & 0 & I_{zz} \end{bmatrix} \tag{30}$$

Therefore, the derived dynamics of DSS are as follows

$$\dot{w}_b = \frac{\bar{\Delta}\,\bar{\omega}}{2\pi} \tag{31}$$

$$\dot{\psi} = \frac{L_b u_2}{K_f} \tag{32}$$

$$\dot{\theta} = \frac{L_b u_3}{K_f} \tag{33}$$

$$\dot{\phi} = \frac{L_b u_4}{K_f + K_w} \tag{34}$$

where, $T_{fw}$is the frictional Torque, $K_f$ is the function of formation properties, $\dot{w}_b$ is the rate of advance of the drilling head in m/sec, also known as the rate of penetration ($R_{op}$), and $W_{ob}$ is the weight on bit and $\bar{\Delta}$ is the rate of penetration per revolution of drill bit is the $\dot{\psi}$ is the Yaw/Pitch velocity, $\dot{\theta}$ is the of azimuth/Inclination velocity and $\dot{\phi}$ is the rate of roll.

From the equations of the dynamics the structure of the model can be shown as in Figure 3.7

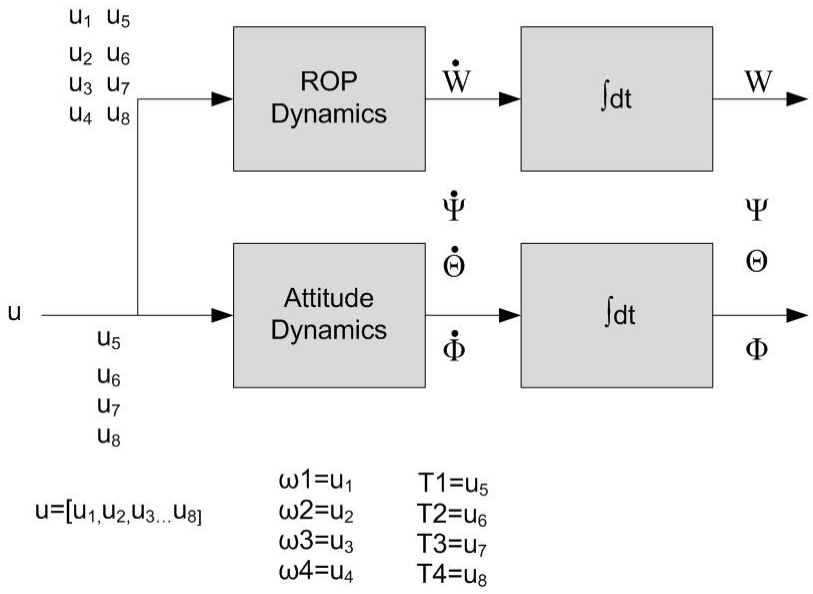


**Figure 3.7: Structure of a DSS Model**

From the Figure 3.7, it can be ascertained that we will be obtaining the ROP, Position, Yaw angle, Azimuth angle and Roll of the BHA.

# CHAPTER 4

# INTERIOR POINT OPTIMIZATION

## 4.1 Introduction

A class of algorithms which solves nonlinear and linear convex optimization (minimizing convex functions over convex sets) problems are called Interior point method. Among these many classes, the prime class of primal-dual path following interior point method is widely accepted and is vigorously used in the MATLAB function ‘fmincon’.

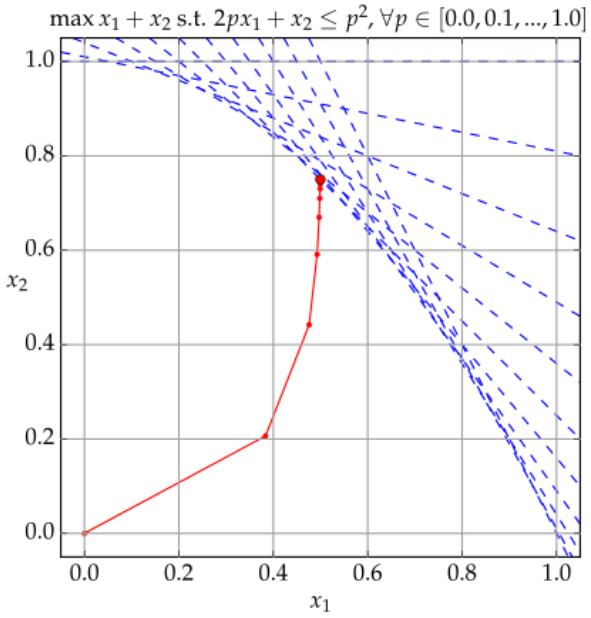


**Figure 4.1: Solution of example LP in Karmarkar's algorithm. Blue lines show the constraints, Red shows each iteration of the algorithm.**

Figure 4.1 is an example of one of the class of interior point methods known as the Karmarkar algorithm which was introduced by Karmarker in the year 1984 for linear programming problems. Form the figure it can be understood that the current guess for the solution does not follow the feasible set boundary but it moves through the interior of the feasible region, thereby increasing the chance of an optimal solution after each iteration and converging to one with a rational data.

## 4.2 Mathematical Review

Describing vectors not only in inertia frame, but also in a body frame is convenient when dealing with drilling objects. The center of the inertial frame is assumed to be the control room location on the oil rig. This is called the earth frame. The inertial frame is defined by $\{X_E, Y_E, Z_E\}$, where $X_E$ points to the geographic north, and $Z_E$ points to the earth center, as shown in Figure **4.2**. The body attitude is described with respect to three virtual body axis, $\{X_B, Y_B, Z_B\}$ located at the body reference point $O_b$. These three reference axis are assumed to be parallel to the inertia axis.

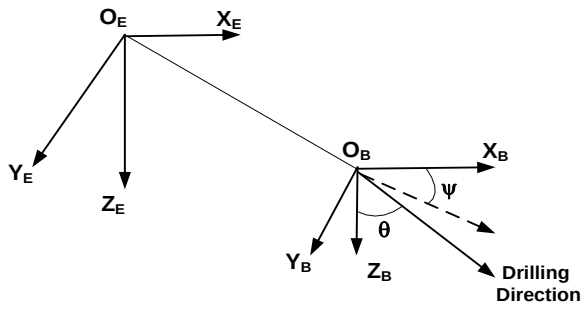


**Figure 4.2: Earth and Body frame.**

When a vector is seen with respect to the earth fixed frame it will be denoted with an $E$ subscript. Likewise if the vector is seen with respect to the body frame will be subscripted with $B$ or b. The BHA position in terms of the inertial frame is represented as the vector

$$\zeta^{T} = [x_E, y_E, z_E] \tag{35}$$

We define $\{U_B, V_B, W_B\}$ to be a body fixed frame. The orientation of the BHA will be described by the rotation of the body fixed frame $\{U_B, V_B, W_B\}$, with respect to the body virtual frame $\{X_B, Y_B, Z_B\}$.

The orientation of the drilling assembly is represented by the three Euler angles, namely the roll angle $\phi$, the Pitch angle $\theta$, and , the yaw angle $\psi$, and presented in the vector

$$\Omega^{T} = [\psi, \theta, \phi]. \tag{36}$$

Initially it is assumed that the body fixed axis $\{U_B,V_B,W_B\}$ is aligned with the inertial frame $\{X_B,Y_B, Z_B\}$. The instantaneous direction of motion is taken to be along $W_B$.

The orientation matrix can be described by the rotational matrix $R_{BE}$ given by

$$R_{BE} = \begin{bmatrix} c\psi s\theta & c\psi c\theta s\phi - s\psi c\phi & c\psi s\theta c\phi - s\psi s\phi \\ s\psi s\theta & s\psi s\theta s\phi + c\psi c\phi & s\psi c\theta c\phi - c\psi s\phi \\ -s\theta & c\theta s\phi & c\theta c\phi \end{bmatrix} \tag{37}$$

The rotational matrix $R_{BE}$ defines the body to inertia axes transformation, where $c\theta$ denotes $\cos\theta$ and $s\theta$ denotes $sin\ \theta$. Let the position of point P w.r.t the body frame be $P_{UVW}$ then the position of the point in the inertia system is given by

$$P_{XYZ} = \begin{bmatrix} x_E \\ y_E \\ z_E \end{bmatrix} + R_{BE}P_{UVW} \tag{38}$$

If we are interested in only the direction of the well bore, we may then ignore the roll rotation of the BHA. In this case $R_{BE}$ is given by

$$R_{BE} = \begin{bmatrix} c\psi s\theta & -s\psi & c\psi s\theta \\ s\psi s\theta & c\psi & s\psi c\theta \\ -s\theta & 0 & c\theta \end{bmatrix} \quad (39)$$

### 4.2.1 Well bore trajectory

Although there are several methods to describe a desired well bore trajectory, we assume without loss of generality the target trajectory is given by table of points indexed by the measured distance $w_b(k)$ along the bore hole. The points need not be uniformly spaced.

The kth target point is given by the vector

$$P_T(k) = [x_E^t(k), y_E^t(k), z_E^t(k), md^t, \theta^t, \psi^t] \quad (40)$$

Where *md* is the measured depth (well bore length).

### 4.2.3 DSS Equations

The experimental Directional Steering System (DSS) is equipped with four motors (5) as shown in Figure 4.3 having a drill bit attached to each of them. These motors are independent from each other for their control giving the user the freedom to manipulate their speed for a precise control on the rate of rock removal and the direction of movement of the drill head. This assembly is attached at the end of the drill string (2) which is responsible for carrying the drilling fluid from the surface to the area of drilling operation. A precise control of the direction of drilling and the optimization of ROP can be achieved by the use of four motors in conjunction with the traditional drilling variables. The direction of rotation is clockwise for the top and bottom motors while it is anti-clockwise for the left and right motors. Pitch action is obtained by decreasing/increasing the speed of the top motor while increasing/decreasing the speed of the bottom motor. The azimuth is obtained

likewise using the left and right motors. A fine management of the drilling process under varied operating constrains and under various drill environment is obtained by the control of the four motors.

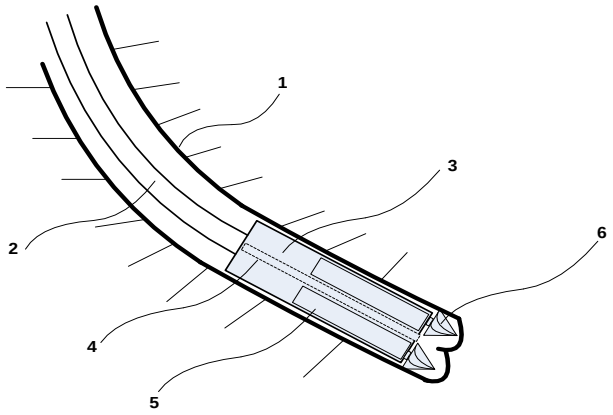


**Figure 4.3: Overview of the drilling assembly**

Let us denote the body rotational angle about $U_B$ by $\theta_1$ , rotational angle about $V_B$ by $\theta_2$ , and the rotational angle about $W_B$ by $\theta_3$.

At a point *k*+1 along the trajectory, the predicted drill position with respect to the body axis is given by

$$\Delta u_b(k+1) = \delta\theta_1[w_b(k+1) - w_b(k)] \quad (41)$$

$$\Delta v_b(k+1) = \delta\theta_2[w_b(k+1) - w_b(k)] \quad (42)$$

$$\Delta w_b(k+1) = w_b(k+1) - w_b(k) \cong R_{op} * t_k \quad (43)$$

Where $t_k$ is the drilling time from the $k^{th}$ point to the $(k+1)^{th}$ point.

The predicted location with respect to the inertia axes will be given by

$$\widehat{\mathrm{P}}_{\mathrm{E}}(\mathrm{k}+1) = \mathrm{P}_{\mathrm{E}}(\mathrm{k}) + \mathrm{R}_{\mathrm{BE}} \begin{bmatrix} \Delta \mathrm{u}_{\mathrm{b}}(\mathrm{k}+1) \\ \Delta \mathrm{v}_{\mathrm{b}}(\mathrm{k}+1) \\ \Delta \mathrm{w}_{\mathrm{b}}(\mathrm{k}+1) \end{bmatrix} \tag{44}$$

### 4.2.3 Drilling Power balance Equations

The drill bit resolves the torque of the motor into two components; a lift force ($F_L$) and a drag torque which is perpendicular to the bit axis ($T_i$). The lift force of the ith motor can be approximated by the relation,

$$\mathrm{F}_{\mathrm{L}} = \mathrm{T}_{\mathrm{i}} \left( \frac{2\pi}{\Delta} \right) \tag{45}$$

Where, $\Delta$ is the feed rate per revolution and $T_i$ is the motor torque.

Depending on the nature of the rock, a minimum amount of energy is required to crush the rock. Rock Specific Energy, $E_{rs}$ in J/m$^3$, is defined as the energy required to crush a unit volume of the rock.

From the energy balance equations, equating the mechanical power by the four motors to the rate of rock crushing, we get

$$\sum_{i=1}^{4} T_i \omega_i + W_{ob} \dot{w}_b = \dot{w}_b A_h E_{rs} \tag{46}$$

Where $\dot{w}_b$ is the rate of advance of the drilling head in m/sec, also known as the rate of penetration ($R_{op}$), and $W_{ob}$ is the weight on bit. Finally, $A_h = \frac{\pi D_h^2}{4}$ is the cross sectional area of well bore, and $D_h$ is hole diameter. The $R_{op}$ is given by

$$R_{op} = \frac{\overline{\Delta}\overline{\omega}}{2\pi} \tag{47}$$

$\overline{\Delta}(t)$ is function of many factors including the rock specific energy, hole $W_{ob}$, the total motor torques, bit geometry, and drilling fluid. However, it can be adjusted using $W_{ob}$ as shown in the following approximate equation

$$\overline{\Delta}(t) = \frac{2\pi \sum_{i=1}^{4} T_i}{A_h Ers - W_{ob}} \tag{48}$$

The bit drag torque is the torque used for crushing the rocks, $T_D$ is approximated by

$$T_D \approx T_i \tag{49}$$

The forces and torques acting on the Bottom Hole Assembly (BHA) can be better described by the following auxiliary inputs:

$$u_1 = F_{L_1} + F_{L_2} + F_{L_3} + F_{L_4} \tag{50}$$

$$u_2 = F_{L_2} - F_{L_4} \tag{51}$$

$$u_3 = F_{L_1} - F_{L_3} \tag{52}$$

$$u_4 = T_{D_1} + T_{D_3} - T_{D_2} - T_{D_4} \tag{53}$$

$u_1$ is related to the total thrust of the four motors, while $u_2$ generates moment responsible for changing the azimuth direction. Similarly, $u_3$ generates the moment for changing the inclination, while $u_4$ generates the torque for the roll motion.

Since all the parameters, except Ers, are directly measurable online, Ers can be estimated. The estimated Value of Ers i.e. $\widehat{E}rs$, is then used during optimization to predict $\dot{w}_b$ during the next control step of DSS as follows

$$\widehat{w}_b(k+1) = f(\tau, \omega, W_{ob}) = \frac{\overline{\Delta}\,\overline{\omega}}{2\pi} = \frac{\sum_1^4 \tau_i\ \overline{\omega}}{A_h \widehat{E}rs - Wob} \tag{54}$$

The lateral rates of penetrations can be approximated by

$$\begin{aligned} \dot{\theta}_1 &= K_{f1} u_2 \\ \dot{\theta}_2 &= K_{f2} u_3 \\ \dot{\theta}_3 &= K_{f3} u_4 \end{aligned} \tag{55}$$

Where $K_{f1}$, $K_{f2}$, and $K_{f3}$ are functions of the formation properties. Now, referring to equations 55 and 54

$$\begin{aligned} \delta\theta_1 &= \dot{\theta}_1 * t_k \\ \delta\theta_2 &= \dot{\theta}_2 * t_k \end{aligned} \tag{56}$$

The Euler angles are driven from the angular velocities of the BHA by the following equation

$$\begin{bmatrix} \dot{\phi} \\ \dot{\theta} \\ \dot{\psi} \end{bmatrix} = \begin{bmatrix} 1 & \sin(\psi)\tan(\theta) & \cos(\psi)\tan(\theta) \\ 0 & \cos(\psi) & -\sin(\psi) \\ 0 & \sin(\psi)\sec(\theta) & \cos(\psi)\sec(\theta) \end{bmatrix} \begin{bmatrix} \dot{\theta}_1 \\ \dot{\theta}_2 \\ \dot{\theta}_3 \end{bmatrix} \tag{57}$$

## 4.3 Drilling Optimization

At each point k, we assume we have a state vector X, and a target position $w_{bt}(k+1)$, and it is required to find the optimal control parameters

The state vector includes

$$X(k) = [t_{total}, w_b, x_E, y_E, z_E, \theta, \psi, \dot{w}_b, \widehat{E}_{rs}] \tag{58}$$

$$U = [\omega_1, \omega_2, \omega_3, \omega_4, T_1, T_2, T_3, T_4, W_{ob}, t_k] \tag{59}$$

### 4.3.1 Optimization cost function

Clearly the objective is to reach the target position $P_E^d(k+1)$ at the end of adjustment step.

The value of $w_b(k+1)$ is obtained as follows

$$\hat{\dot{w}}_b(k+1) = f(\tau, \omega, W_{ob}) = \frac{\overline{\Delta}\,\overline{\omega}}{2\pi} = \frac{\sum_1^4 \tau_i\ \overline{\omega}}{A_h \hat{E}rs - Wob} \tag{60}$$

$$\hat{w}_b(k+1) = w_b(k) + t_k f(\omega, W_{ob}) \tag{61}$$

The optimal values of control parameters are obtained by minimizing the cost function

$$J = (\hat{P}_E(k+1) - P_E^d(k+1))^T\ \Gamma_1\ \left(\hat{P}_E(k+1) - P_E^d(k+1)\right) + U^T\ \Gamma_2\ U \tag{62}$$

Where $U$ is the input parameters vector, $\Gamma_1$ and $\Gamma_2$ are positive semi-definite weighting matrices, $\hat{P}_E(k+1)$ is the predicted position and $P_E^d(k+1)$ is the target position.

Figure 4.4: Block Diagram of the control system shows the control architecture of the IPO optimization scheme and Figure 4.5 explains the algorithm involved in the control of the system using IPO

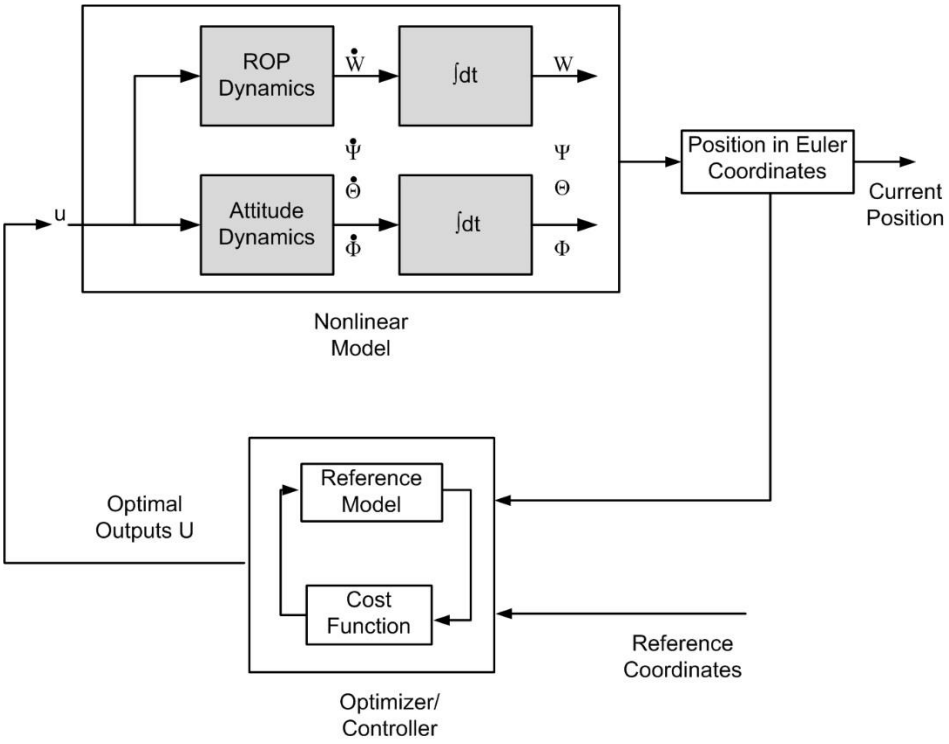


**Figure 4.4: Block Diagram of the control system**

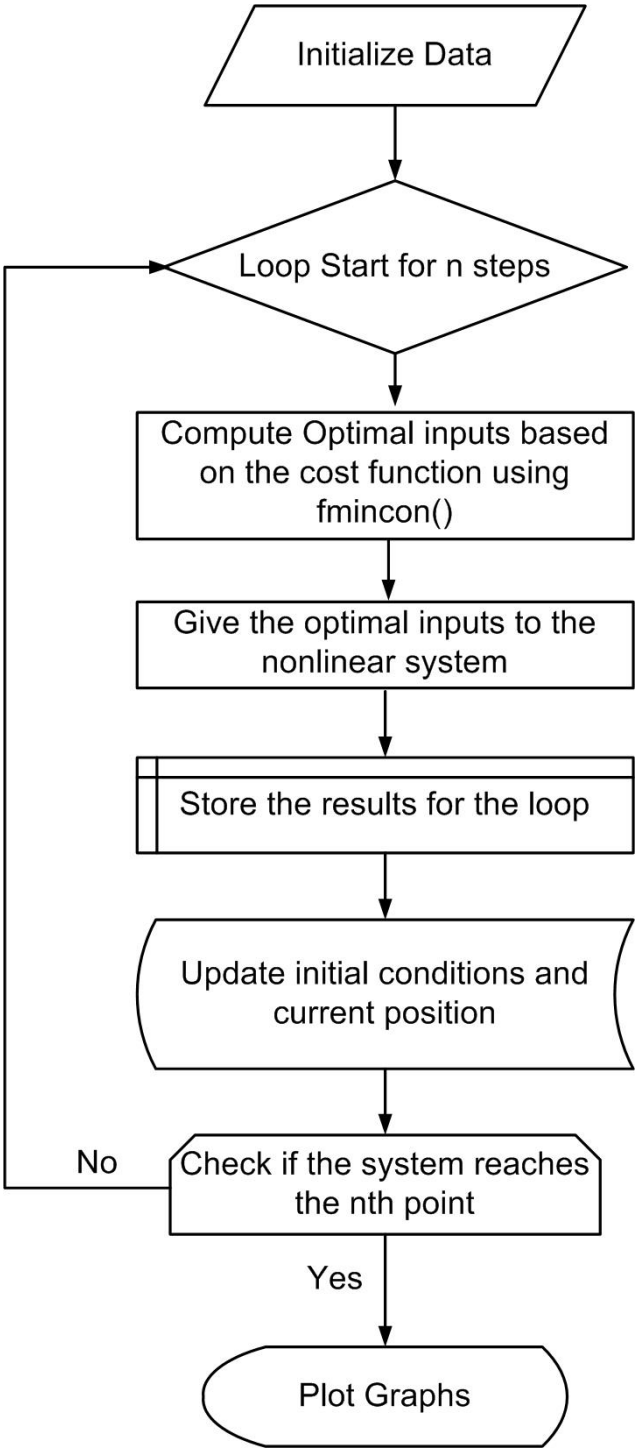


**Figure 4.5: Control algorithm using the IPO technique**

## 4.4 Simulation

The proposed optimization method is applied to follow the drilling trajectory shown in figure. This section of a well has a total measured length of 1318, and TVD =254 meters. The section starts by a 30 degree inclination, and proceeds approximately in two continuous build zones to reach almost horizontal drilling (87.9 degree inclination). RSE are assumed to be unknown, but estimated based on the achieved ROP during the previous control step.

The actual and target trajectory is as shown in Figure 4.6.

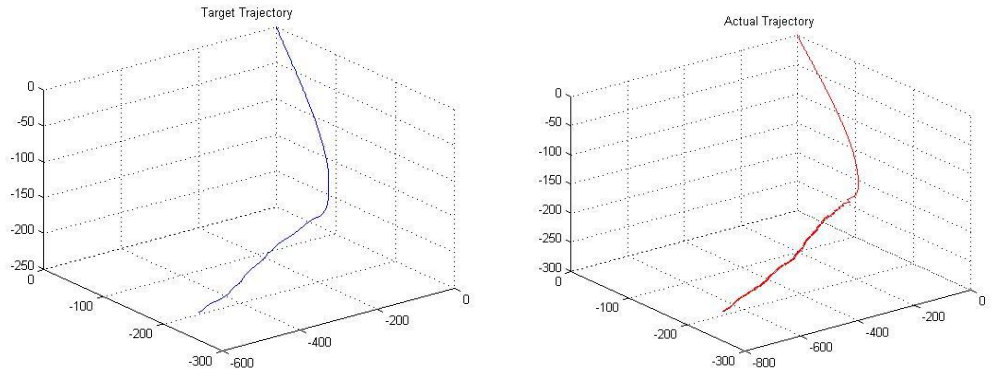


**Figure 4.6: Target Trajectory and Actual Trajectory**

During simulation $\Gamma_1$ is taken to be unit matrix. Two control strategies were simulated. In the first case $\Gamma_2$ was taken to be zero, i.e. no cost for the drilling effort. The drilling time came to be 12.1679 hours with a maximum deviation of 0.13 meters. In the second case, the cost of drilling time is considered. The drill time is reduced to 4.7323 hours with a tracking error reaching a maximum value of 22.9 meters. It was observed that increasing the cost of time beyond this value did appreciably reduce the drilling time, but compromises in tracking accuracy. The results can be listed as in Table 4.1

**Table 4.1: Comparison of results with and without time optimization**

| Factor | With Time and Error Cost ($\Gamma_1 \neq 0, \Gamma_2 \neq 0$) | With Error Cost ($\Gamma_1 \neq 0, \Gamma_2 = 0$) |
|---|---|---|
| Drill Time (in hours) | 4.73 | 12.16 |
| Maximum Deviation (in meters) | 22.9 | 0.13 |
| Mean Torque (in Nm) | 272.91 | 91.182 |
| Mean RPM | 49.363 | 46.49 |
| Average ROP (in m/min) | 4.64 | 1.55 |

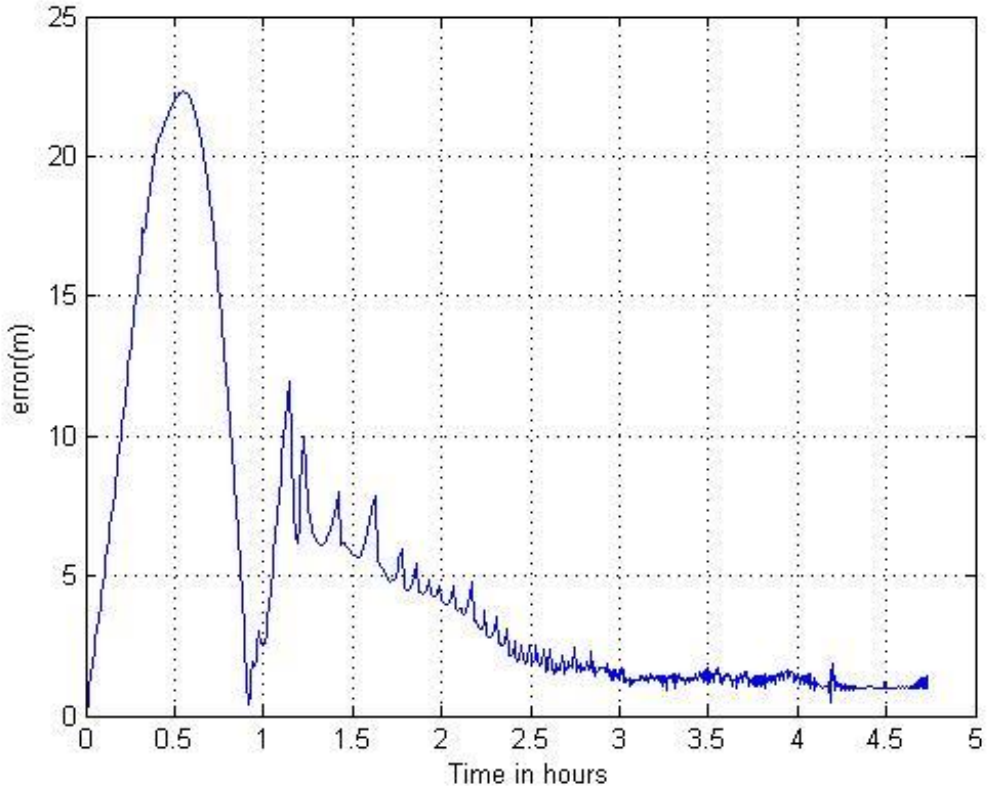


**Figure 4.7: Deviation from the path in meters (error)**

Figure 4.7 shows the amount of deviation from the reference trajectory obtained during the simulation. From the graph it can be deduced that the mean error is 4.99 meters which is low and the system follows a smooth trajectory. Hence an optimal solution is reached having high accuracy with minimum time for drilling. The variation is RSE based on the depth of the land profile is as shown in Figure 4.8. This acts as an unmeasured disturbance to the system.

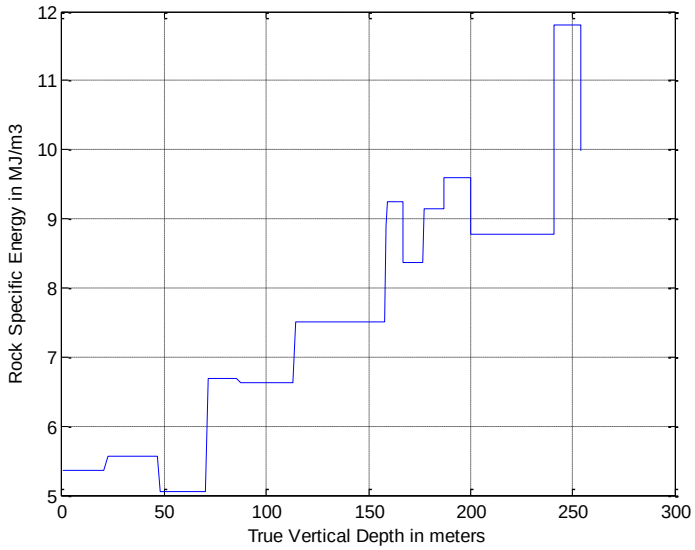


**Figure 4.8: Variation in Rock specific energy**

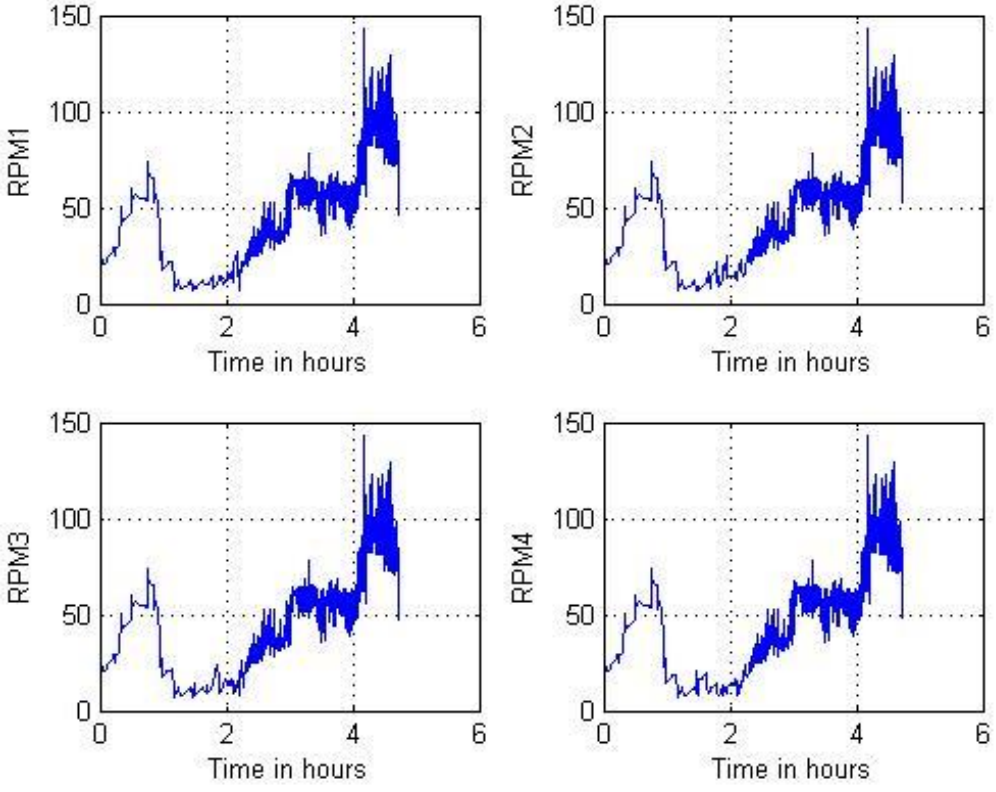


**Figure 4.9: Variation in RPM of the Four Motors during drilling**

The variation in RPM for each individual drill bit is shown in Figure 4.9. From the figure it can be observed that RPM of the motors are almost equal with respect to each other during the drill operation. However, the change in the ground resistance as shown in Figure 4.8 results in the corresponding change in the RPM. When rock specific energy increases, the RPM increases and when it decreases, the RPM decreases.

Figure 4.10 shows the corresponding torque values. It could be conferred that the torque in the adjacent motors are equal at each step in order to prevent the system from rolling.

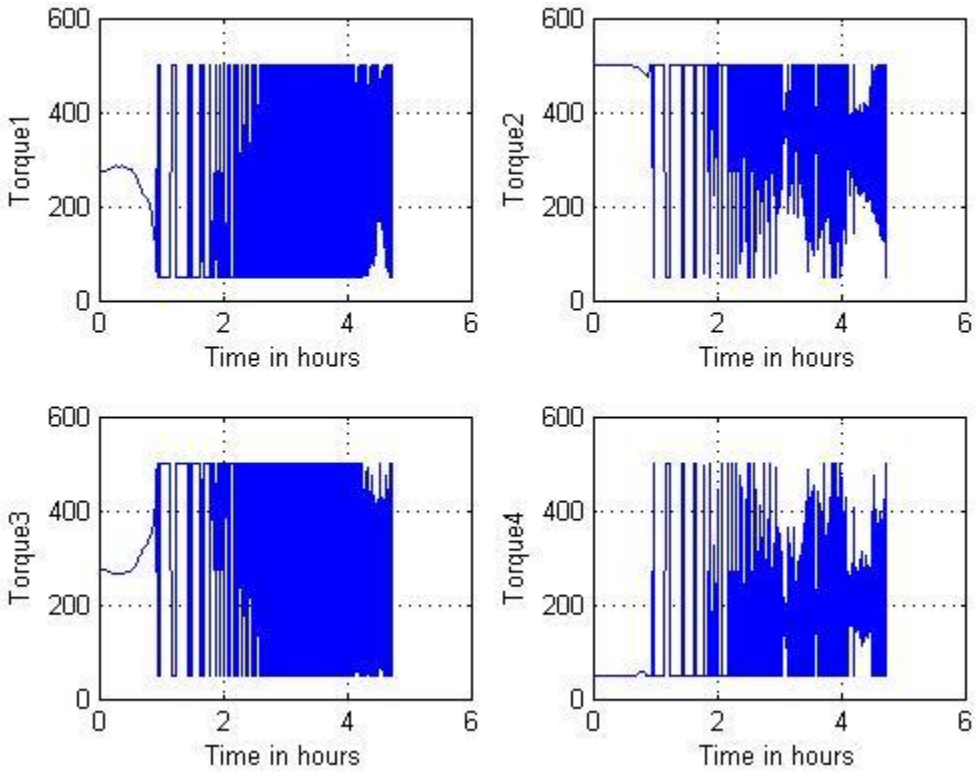


**Figure 4.10: Variation in Torque of the Four Motors during drilling**

The minimization of the cost function in equation is performed using Matlab constraint minimization function “fmincon”, by the interior-point algorithm. The lower and upper bounds on the control values are given in Table 4.2

**Table 4.2: Upper and the lower bound for the control parameters**

| Parameter | Min | Max |
|---|---|---|
| $\tau_1$ | 50 Nm | 500Nm |
| $\tau_2$ | 50 Nm | 500Nm |
| $\tau_3$ | 50 Nm | 500Nm |
| $\tau_4$ | 50 Nm | 500Nm |
| $\omega_1$ | 4π rpm | 250 rpm |
| $\omega_2$ | 4π rpm | 250 rpm |
| $\omega_3$ | 4π rpm | 250 rpm |
| $\omega_4$ | 4π rpm | 250 rpm |
| $W_{ob}$ | 500 kg | 5000 kg |
| $t_k$ | 20 sec | 3600 sec |

# CHAPTER 5

# MODEL PREDICTIVE CONTROL

## 5.1 Introduction

Another important type of controller presented is the model predictive controller (MPC). In order to compare the performance of the DSS system, a strategy of fixed time and fixed distance control techniques were adopted. The Interior Point method of optimization (chapter 4) uses the fixed distance algorithm while the MPC has a fixed time base for all the computations along the trajectory line. The method of execution could be described as obtaining a linear estimated model of the system at each step and applying an MPC on the model to reach the desired location. This can be understood by studying the program flow algorithm (Figure 5.1) and observing the control block diagram of the system (Figure 5.2).

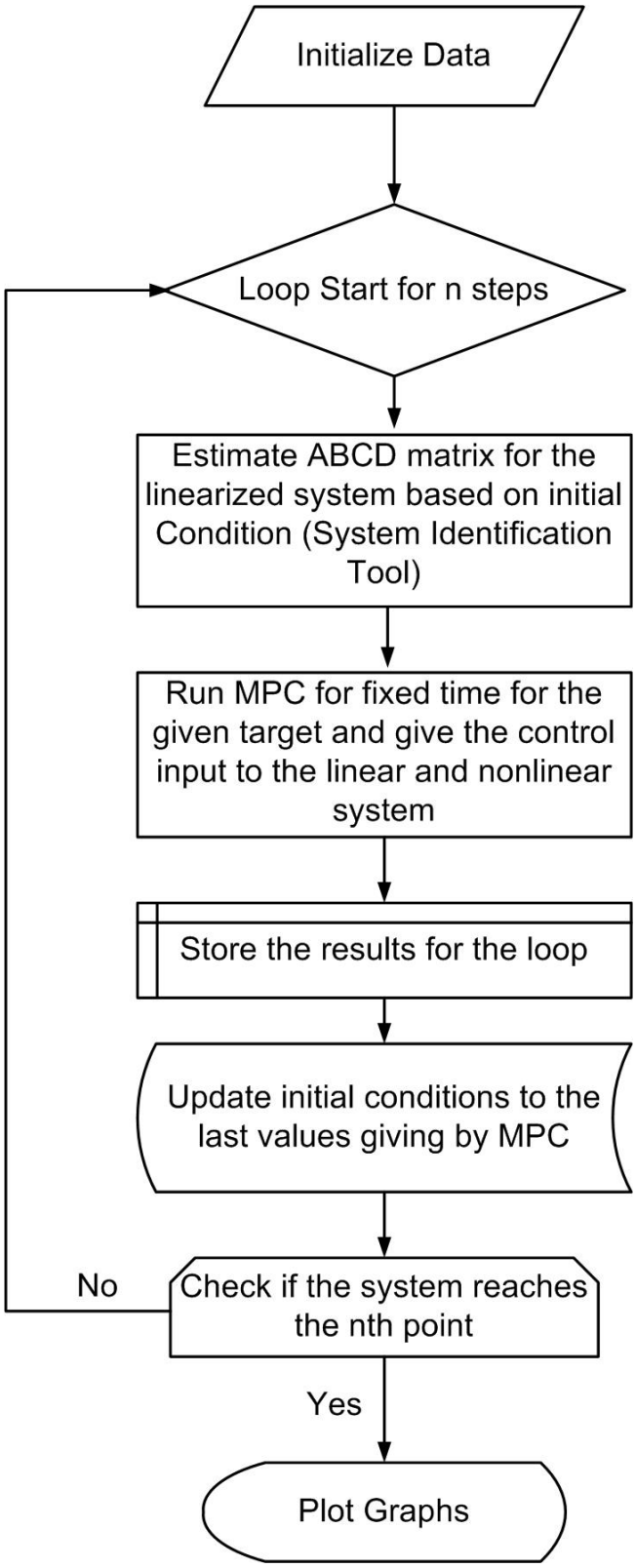


**Figure 5.1: Program flow algorithm of the DSS system**

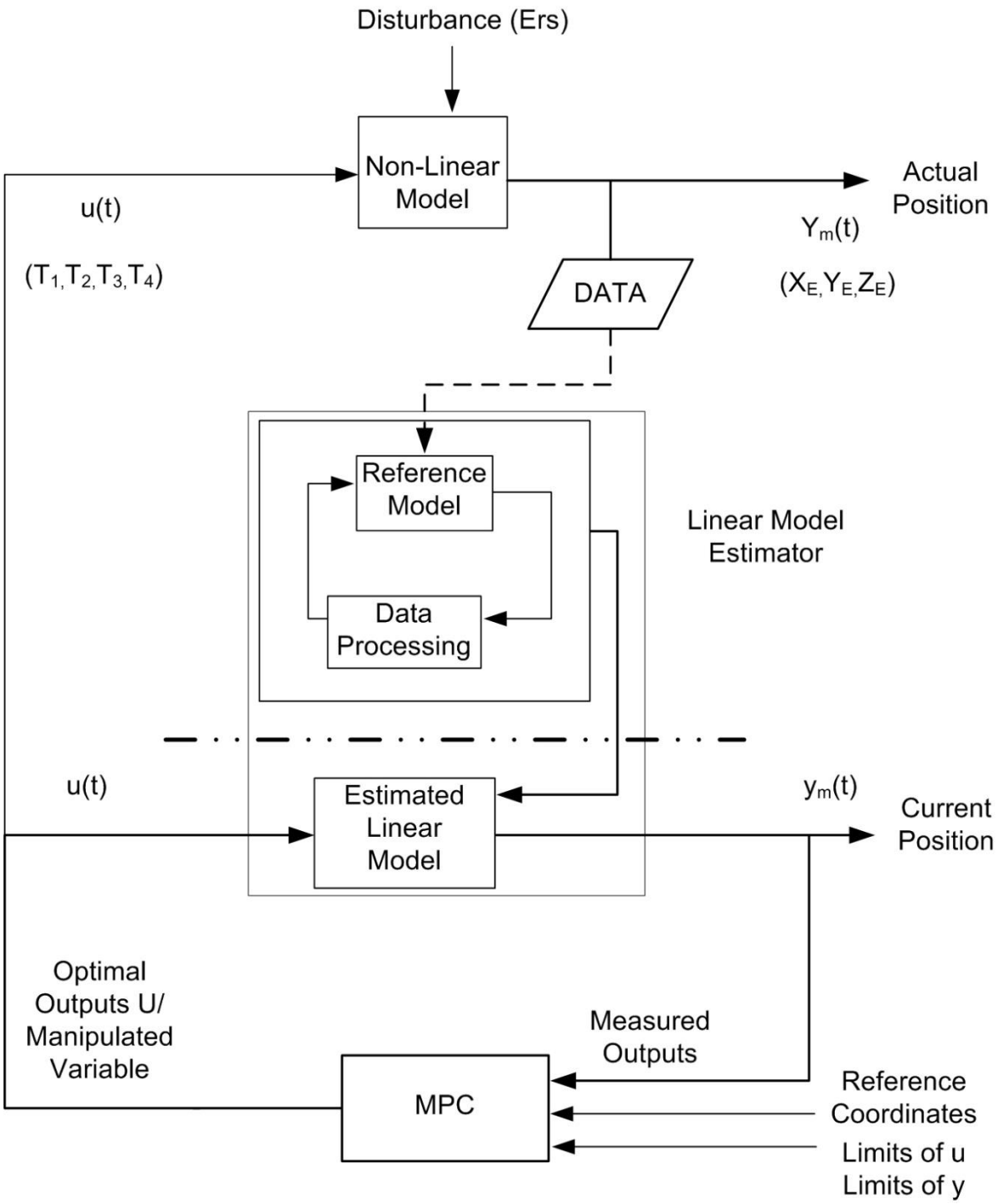


**Figure 5.2: Control Block diagram of the DSS system**

From Figure 5.2, it can be observed that at each step the linear model estimation algorithm is run, which formulates a linear state space model based on the input-output sample data of the system at that instance. The DATA block contains all the data such as rock specific

energy, current and desired trajectory, information about the states of the system etc. This estimated linear model is then controlled by the MPC to generate the desired trajectory based on the manipulated variables given to the system by the MPC. These control signals from the MPC are given to the non-linear system and a step change in position is obtained for the system. This process repeats after a fixed time interval till the system reaches the final desired position. The underlying mathematical equations governing the control and estimation of the system is explained in the following sections.

## 5.2 State-space Model Predictive Control

It is a relatively recent type of controller design technique that makes explicit use of a model to obtain a control signal. In other words, the MPC objective is to compute the future values of the control signal or the manipulated variables in order to optimize the future behavior of the output variable of the plant and minimize the objective function [Holkar et al (2010)] shown in Eqn. 63, subject to constraints on input and output variables.

$$\min\left\{\sum_{k=0}^{N-1}\|y(t+k) - r(t)^2\| + \rho\|u(t+k) - u(t)\|^2\right\} \quad (63)$$

This optimization is performed within a limited time window by giving the plant information or the plant model at the start of the window. This methodology of obtaining the control signal is known as Receding Horizon Principle. The performance of the controller depends on how well the dynamics of the system are captured by the plant model to be used in the design of controller. The main reason for the popularity of MPC is its ability to handle constraints on both input and output variables and the ease with which it provides the optimization.

The strategy called ‘Receding Horizon’ wherein the horizon is moved one step towards the future but involves the application of only the first control signal from the computed control sequence is shown in Figure 5.3.

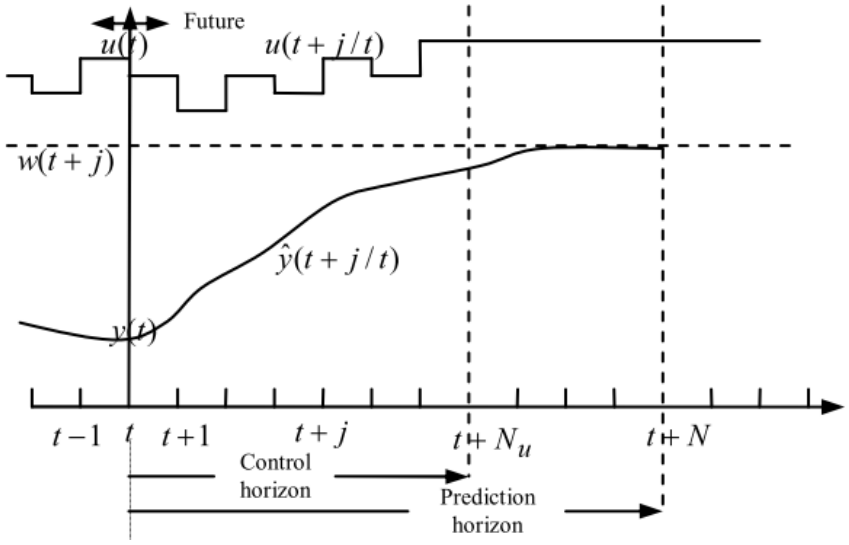


**Figure 5.3: Receding Horizon Philosophy**

The process model calculates the predicted future outputs $\hat{y}(t+j)$ for the prediction horizon ‘N’ at each time instant. The calculation of the future control signals for the control horizon ‘$N_u$’ is computed to minimize the objective function. However the current signal u(t) is sent to the process. At the next sampling instant y(t+1) is measured and the same process is repeated wherein now the control signal u(t+1) is calculated using receding horizon concept and sent to the process.

### 5.2.1 Models used in MPC Design

MPC Control is done in a variety of ways which differ on the basis of the model that is used in the control design. During the initial times when MPC was developed, FIR models and step response models were used. The usage of these models for MPC design is referred to as Dynamic Matrix Control. The choice of selection of one of these two models is based on the

application they are used for. FIR models are used for plants which are stable and those which require the models to be of large order whereas step response models can be used for both unstable as well as stable plants. However in recent times, it is the used of state-space models for MPC formulation that has become very popular. In this work also, the state-space models in discrete time are used for MPC Control and the principle it is based on is known as the Receding Horizon Control.

### 5.2.2 Optimization

For optimization, we need a condition to decide on how to achieve the control objective using MPC control. One basic rule is to measure the difference between the target value and the actual process value in terms of an objective function and then finding ways and means to optimize the control action in reducing the cost function to as minimum value as possible. However, all this is to be done inside the prediction horizon.

Let us assume that $r(k_i)$ is the desired value of the output variable at sample time $k_i$ (discrete case). The goal would now be to find best control action in terms of ΔU which minimizes the gap between desired value and actual value of the process variable being controlled. Consider the data vector containing the desired value, is given by Eqn. 64.

$$R_s^T = \overbrace{[1\ 1\ \dots 1]}^{N_p} r(k_i) \tag{64}$$

The cost function J can be defined as given in Eqn.65.

$$J = (R_s - Y)^T (R_s - Y) + \Delta U^T \bar{R} \Delta U, \tag{65}$$

The first term is for minimizing the errors between set-point signal and the predicted output and the second term is for the consideration to be given to the size of ΔU during the

minimization of objective function J. $\overline{R}$ is a diagonal matrix in the form that $\bar{R} = r_w I_{Nc\,x\,Nc}$($r_w \geq 0$) where $r_w$ is used as a tuning parameter for the desired closed-loop performance.

When $r_w$ is zero, the objective function (65) is seen as the position wherein we are not interested in what ΔU is (large or small) but our objective is to reduce the error between the desired value and the actual value given by $(R_s - Y)^T(R_s - Y)$ to the least possible value. When $r_w$ is large, the function (65) is seen as the situation where we are concerned about how large or small ΔU is and at the same time we would very carefully work towards reducing the error between desired and the actual value. We have the predictor equation for output Y given by Eqn.66 as,

$$Y = Fx(k_i) + \Phi\Delta U \tag{66}$$

For the optimal value of ΔU that will minimize J, we substitute (66) in (65), and obtain the expression of J as:

$$J = \left(R_S - Fx(k_i)\right)^T\left(R_S - Fx(k_i)\right) - 2\Delta U^T\Phi^T\left(R_S - Fx(k_i)\right) + \Delta U^T(\Phi^T\Phi + \bar{R})\Delta U \tag{67}$$

On taking the first derivative of the cost function J given in (67), with respect to control signal ΔU we obtain equation 68:

$$\frac{\partial J}{\partial \Delta U} = -2\Phi^T\left(R_S - Fx(k_i)\right) + 2(\Phi^T\Phi + \bar{R})\Delta U, \tag{68}$$

The necessary condition of the minimum J is obtained as $\frac{\partial J}{\partial \Delta U} = 0$, from which we get the optimal solution for the control signal as,

$$\Delta U = (\Phi^T \Phi + \bar{R})^{-1} \Phi^T \left(R_S - Fx(k_i)\right) \tag{69}$$

With the assumption that $(\Phi^T \Phi + \bar{R})^{-1}$ exists. The matrix $(\Phi^T \Phi + \bar{R})^{-1}$ is called the Hessian Matrix. Note that $R_s$ is a data vector that contains the set point information expressed as,

$$R_s^T = \overbrace{[1\ 1\ \ldots 1]^T}^{N_p} r(k_i) = \bar{R}_s r(k_i), \text{ where } \bar{R}_s = \overbrace{[1\ 1\ \ldots 1]^T}^{N_p} \tag{70}$$

The link of the optimal solution of the control signal to the set-point signal $r(k_i)$ and the state variable $x(k_i)$ is via the following equation:

$$\Delta U = (\Phi^T \Phi + \bar{R})^{-1} \Phi^T \left(\bar{R}_s r(k_i) - Fx(k_i)\right) \tag{71}$$

Hence the model predictive control problem is to minimize the cost function modified as:

$$\left\{\sum_{k=0}^{N-1} \|y_{t+k} - r(t)\|^2 + \rho \|u_{t+k} - u_r(t)\|^2\right\} \tag{72}$$

subject to constraints on input and output given as: $u_{min} \leq u_{t+k} \leq u_{max}$ ,$y_{min} \leq y_{t+k} \leq y_{max}$.

MATLAB provides an in-built toolbox called Model Predictive Control Toolbox [Bemporad (2012a)] for a system whose model is given in state-space form. In this work, the controller is designed for the third order state-space model of Directional Drilling System estimated by sub-space identification.

## 5.3 State-space System Identification

It is the type of system identification to estimate the state-space models from the experimental data. There are two methods of system identification by which state-space models can be computed based on experimental data. They are subspace identification and prediction error method.

The subspace identification method Huerta et al (2012) is a non-iterative method of estimating discrete time state-space models and prediction error method is an iterative estimation method that minimizes prediction error. These models can be estimated in MATLAB environment using the commands *n4sid* and *pem*. The general format of the discrete state-space model is given in Eqn. 73 as:

$$x(t + Ts) = Ax(t) + Bu(t) + Ke(t) \quad (73)$$

$$y(t) = Cx(t) + Du(t) + e(t)$$

Where 'x' represents the state vector, 'u' represents the input vector and 'y' represents the output vector. A, B, C, D and K matrices are state-space matrices estimated by system identification. They represent the system dynamics and are known as model coefficients.

### 5.3.1 Subspace Identification

The subspace identification method was developed in 1980's and is based on the Singular Value Decomposition (SVD) and the QR factorization [Katayama (2005)]. Some of the key features of subspace identification are [Overschee et al (1994)]:

1) It gives the minimum realization of the model in the state-space form.

2) The state-space model is estimated using the experimental data and doesn't require to construct a priori parameterization. The only detail required for subspace identification is

the model order, which is obtained by inspecting the dominant singular values of a matrix which is calculated during the identification process.

3) Subspace Identification is a non-iterative procedure and do not require any non-linear optimization. Hence they do not pose problems related to convergence, local minima or sensitivity to the parameter values (initial values). Also they have less computation as compared to other techniques like Prediction Error Minimization (PEM) [Ljung (1987)] method.

4) There is no criterion for the initial condition to be mentioned and can be considered as zero.

The subspace identification algorithms present the next common steps [Favoreel et al (1998)]:

Construct the Hankel matrices for output and input, using the output and input measurements, $\{u_k\}_{k=1}^{N}$ and $\{y_k\}_{k=1}^{N}$ as given by Eqn. 74.

$$U_{0|k-1} = \begin{bmatrix} u(0) & u(1) & \dots & u(N-1) \\ u(1) & u(2) & \dots & u(N) \\ \vdots & \vdots & \ddots & \vdots \\ u(k-1) & u(k) & \dots & u(N-k+2) \end{bmatrix} \quad (74)$$

The block Hankel matrix for output data ($Y_{0|k-1}$) is constructed in a similar fashion as in Eqn. 74 and realization of QR decomposition is done by using these matrices. To find the extended observability matrix, the singular value decomposition (SVD) is performed on the R-component which has a low rank.

The two state-space identification methods differ from each other in terms of how these steps are computed. After these three common steps, the procedure followed for determining the matrices A, B, C, D and K is completely different and varies according to the method used .

The subspace identification is based on the work done by Van Overschee and De Moor .

For notational convenience, let p and f denote the past and future respectively. Hence we define the past-data as $U_p$: = $U_{0|k-1}$ and $Y_p$: = $Y_{0|k-1}$ and future-data as $U_f$ : = $U_{k|2k-1}$ and $Y_f$ : = $Y_{k|2k-1}$. The joint past data is denoted by $W_p := \begin{bmatrix} U_p \\ Y_p \end{bmatrix}$ and the joint future data is denoted by $W_f := \begin{bmatrix} U_f \\ Y_f \end{bmatrix}$.

Let the LQ decomposition be given by

$$\begin{bmatrix} U_f \\ W_p \\ Y_f \end{bmatrix} = \begin{bmatrix} R_{11} & 0 & 0 \\ R_{12} & R_{22} & 0 \\ R_{13} & R_{23} & R_{33} \end{bmatrix} \begin{bmatrix} \bar{Q}_1^T \\ \bar{Q}_2^T \\ \bar{Q}_3^T \end{bmatrix} \tag{75}$$

where $R_{11} \epsilon R^{km \times km}$, $R_{22} \epsilon R^{k(m+p) \times k(m+p)}$ and $R_{33} \epsilon R^{kp \times kp}$ are diagonal elements and $Q_i$ (i=1, 2, 3) are orthogonal matrices.

Let the oblique projection of $Y_f$ onto joint-past $W_p$ along future $U_f$ is given by,

$$\xi = \hat{E}_{||Uf}\{Y_f | W_p\} = R_{32} R_{22}^{+} W_p \tag{76}$$

where $(.)^+$ denotes the pseudo inverse. We can show that $\xi$ can be factored as a product of extended observability matrix $O_k$ and future state vector $X_f$ := [ x(k) . . . x(k+N-1)] $\epsilon R^{nxN}$. It thus follows that,

$$\xi = O_k X_f = R_{32} R_{22}^{+} W_p \quad (77)$$

Suppose the Singular-value decomposition (SVD) of ξ is given by

$$\xi = U \sum V^T \quad (78)$$

with rank(∑) = n. Thus we can take the extended observability matrix as

$$O_k = U \sum^{1/2} \quad (79)$$

Substituting the value of ξ and $O_k$ from Equations 78 and 79 in Equation 77, it follows that the value of state vector $X_f$ is obtained as

$$X_f = O_k^{+} \xi = \sum^{1/2} V^T \quad (80)$$

We define the following matrices with N-1 columns as,

$$\bar{X}_{k+1} := [x_{k+1} \quad \dots \quad x_{k+N-1}] \quad (81)$$

$$\bar{X}_k := [x_{k+1} \quad \dots \quad x_{k+N-2}] \quad (82)$$

$$\bar{U}_{k|k} := [u_k \quad \dots \quad u_{k+N-2}] \quad (83)$$

$$\bar{Y}_{k|k} := [y_k \quad \dots \quad y_{k+N-2}] \quad (84)$$

By using the least square method for solving the system of linear equations, the A, B, C and D matrices are obtained.

$$\begin{bmatrix} \bar{X}_{k+1} \\ \bar{Y}_{k|k} \end{bmatrix} = \begin{bmatrix} A & B \\ C & D \end{bmatrix} \begin{bmatrix} \bar{X}_k \\ \bar{U}_{k|k} \end{bmatrix} \quad (85)$$

However, the state-space model based on subspace identification can be computed using the built-in MATLAB command called *'n4sid'*.

The results obtained from subspace identification using MATLAB command *n4sid* for the first step are:

$$A_n = \begin{pmatrix} 0.01958 & -0.0117 & -0.02408 \\ 0.08725 & -0.03265 & -0.1395 \\ -0.01364 & 0.149 & -0.05983 \end{pmatrix},$$

$$B_n = \begin{pmatrix} -1.731e-05 & -1.274e-05 & -6.636e-06 & -7.858e-07 \\ -8.214e-05 & 9.572e-05 & -7.567e-05 & -5.529e-05 \\ -0.0001547 & 0.0001898 & 3.239e-05 & -2.419e-05 \end{pmatrix}$$

$$C_n = \begin{pmatrix} 355.2 & 25.57 & -38.7 \\ 94.13 & -86.72 & 24.68 \\ 254.6 & -12.91 & 55.25 \end{pmatrix}, \quad D_n = \begin{pmatrix} 0 & 0 & 0 & 0 \\ 0 & 0 & 0 & 0 \\ 0 & 0 & 0 & 0 \end{pmatrix},$$

$$Kn = \begin{pmatrix} 0.0007856 & -0.0002392 & 0.001084 \\ 0.0005548 & -0.005831 & 0.003361 \\ -0.001106 & 0.001333 & 0.003955 \end{pmatrix}$$

Status:

Estimated using N4SID on time domain data "mydata".

Fit to estimation data: [87.22; 81.5; 86.23] %

### 5.3.2 Prediction Error Minimization Method

Prediction Error Methods is a broad family of parameter estimation methods that is applied to quite arbitrary model parameterizations. These methods are closely related to Maximum Likelihood method, originating from Fisher (1912) and were used for the computation of dynamical models and time series by Jenkins (1970) and Astrom (1965).

The basic idea behind the prediction error approach is very simple:

1) Describe the model as a predictor of the next output.

$$\hat{y}_m(t|t-1) = f(Z^{t-1}) \tag{86}$$

Where $\hat{y}_m(t|t-1)$ denotes the one-step ahead prediction of the next output and *f* is arbitrary function of the past observed data.

2) Parameterize the predictor in terms of finite dimensional parameter vector θ:

$$\hat{y}_m(t|\theta) = f(Z^{t-1}, \theta) \tag{87}$$

3) Determine an estimate of θ (denoted as $\hat{\theta}_N$) from the model parameterization and the observed dataset $Z^N$ so that the error between y and $\hat{y}$ is minimized.

In this way, the unknown model parameters can be estimated using iterative prediction error minimization method. MATLAB has a built-in command called *'pem'* to estimate the state-space model based on prediction error minimization principle.

And the results obtained from prediction error method using MATLAB command *pem* for the first step are:

$$\mathrm{A_n} = \begin{pmatrix} 0.1092 & 0.07424 & -0.2356 \\ -0.7234 & -0.9205 & 0.8146 \\ 1.015 & -0.09664 & -2.809 \end{pmatrix},$$

$$\mathrm{B_n} = \begin{pmatrix} 6.09e-05 & 0.0001099 & -5.343e-05 & -0.0001203 \\ 0.0003067 & -0.0009773 & 6.946e-05 & 0.0009732 \\ 0.0006567 & 0.001586 & -0.0007851 & -0.001918 \end{pmatrix}$$

$$\mathrm{C_n} = \begin{pmatrix} -340.3 & 13.63 & 47.87 \\ -77.48 & -92.51 & -0.3671 \\ -236 & -38.8 & -23.02 \end{pmatrix}, \quad \mathrm{D_n} = \begin{pmatrix} 0 & 0 & 0 & 0 \\ 0 & 0 & 0 & 0 \\ 0 & 0 & 0 & 0 \end{pmatrix},$$

$$\text{Kn} = \begin{pmatrix} -0.0199 & 0.01349 & -0.02841 \\ 0.03759 & -0.1513 & 0.01619 \\ 0.07574 & 0.1667 & -0.2022 \end{pmatrix}$$

Status:

Estimated using SSEST on time domain data "mydata".

Fit to estimation data: [88.97; 89.38; 88.55] %

It is interesting to note that the accuracy of the estimated model based on the generated data is higher for a PEM in comparison to N4SID. Therefore in our simulations we used PEM via a MATLAB function called 'ssest()'

## 5.4. Results

The simulation is run subjected to the constraints listed in Table **6.1**. The inputs to the system are Torques of the four motors and the outputs are the position ($x_E$, $y_E$ and $z_E$). The states are the wd, $\psi$ and $\Theta$. Roll is considered to be zero.

The system is initialized with states at zero and input torques at 100N. We select the values of the variables used in the equations 31, 32, 33 and 34 as listed in the Appendix. The trajectory selected for the simulation consist of 490 equally distant trajectory points. The simulation is run in discreet form moving along the target one step at a time. During each step, a bounded random set of input data is given to the reference model and the corresponding output is recorded. We select the sample size of the input and output data of 100. Next, we use the sample data and generate a linear estimated model using the System Identification Function 'ssest()'.

Then we design an MPC based on this estimated linear model with a sample time of 0.1 prediction horizon of 8 and a control horizon of 3. We run the linear system controlled by this MPC for a time duration of 60 sec. The MPC generates the optimal control signal to control the linear model which are simultaneously given to the non-linear model and the results are stored. This process is repeated for 490 steps with the initial conditions being updated to the last values at every step. The results are then plotted using the saved data.

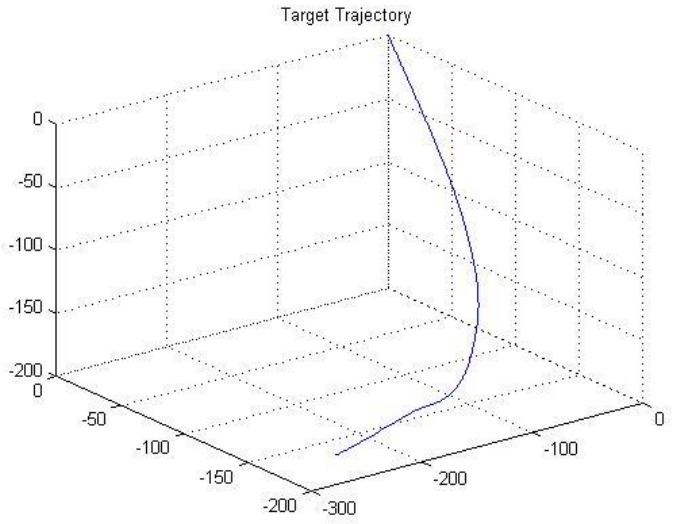


**Figure 5.4: Target Trajectory**

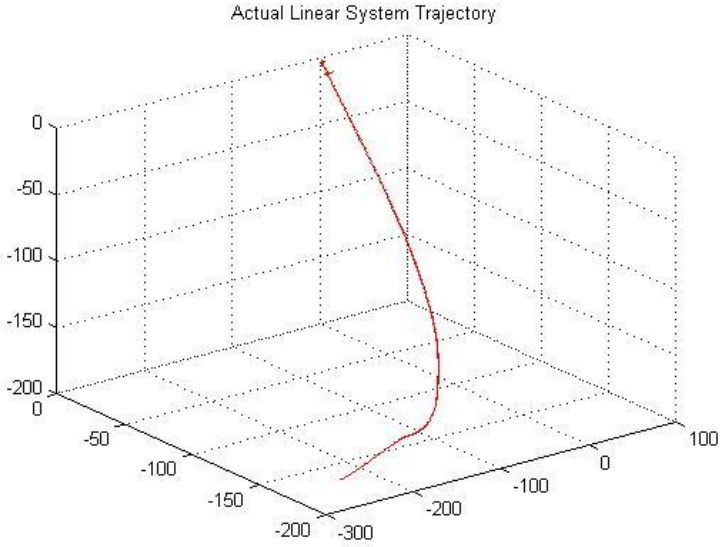


**Figure 5.5: Actual Linear System Trajectory**

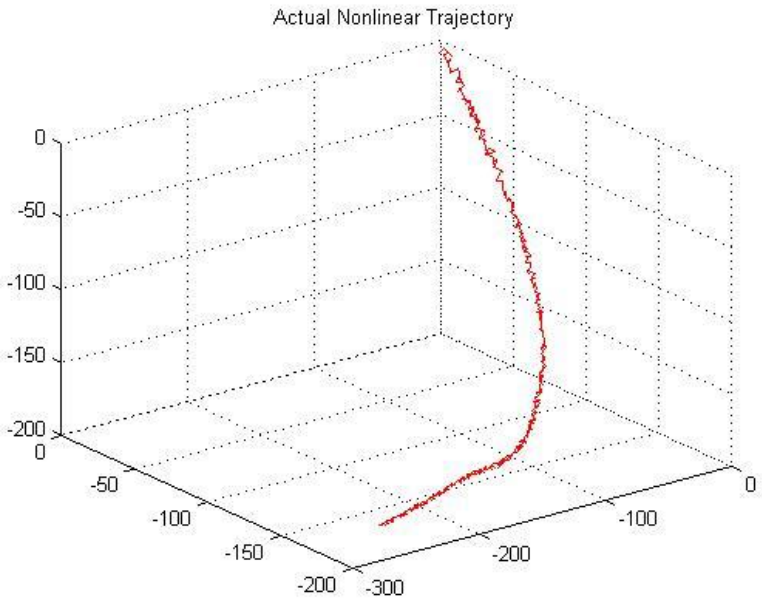


**Figure 5.6: Actual Nonlinear System Trajectory**

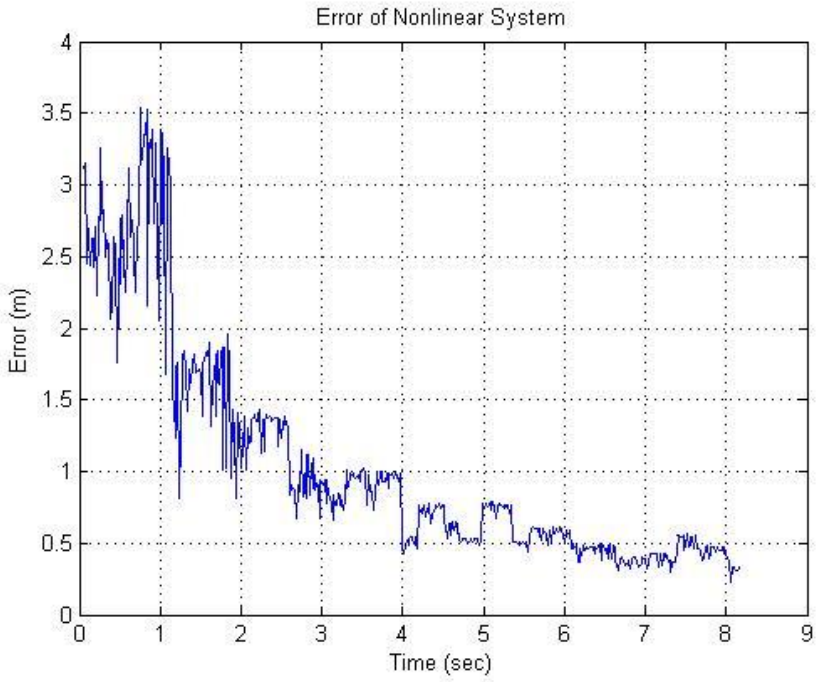


**Figure 5.7: Error in Trajectory of a non-Linear System**

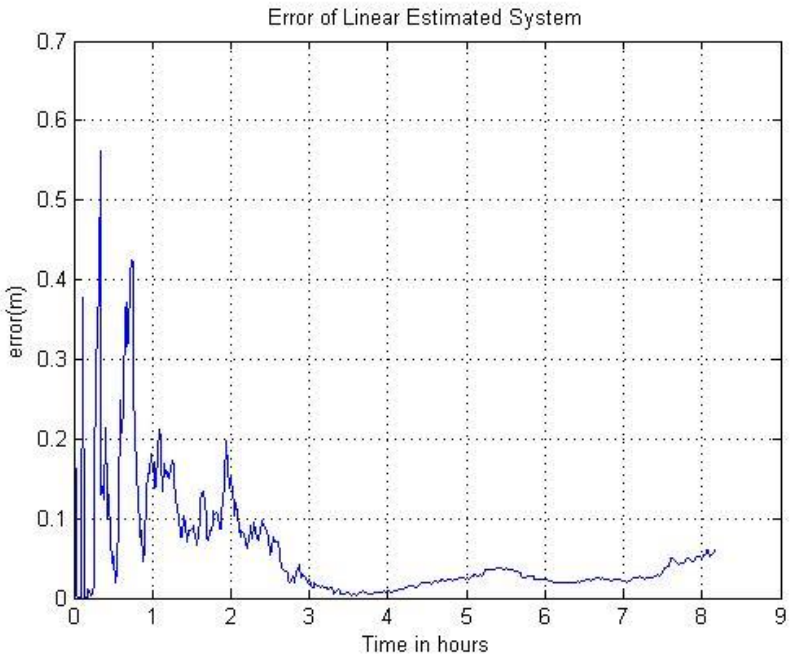


**Figure 5.8: Error in Trajectory of a Linear System**

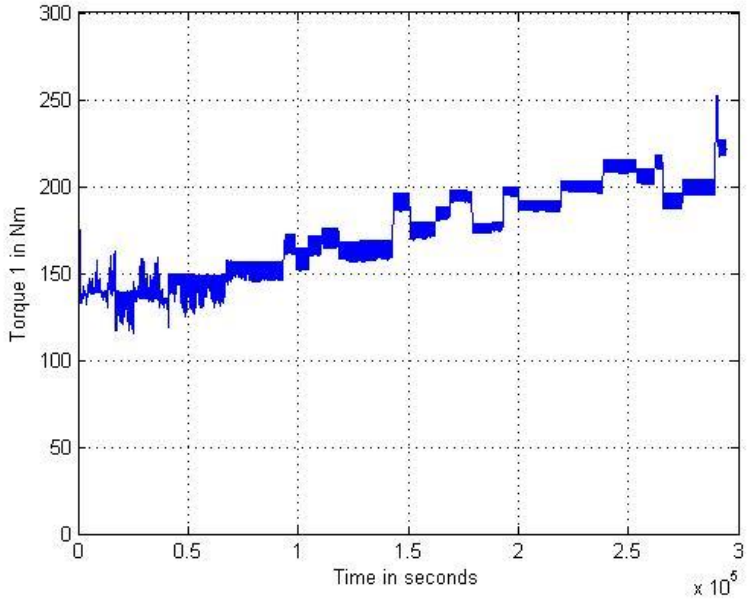


**Figure 5.9: Torque of motor 1**

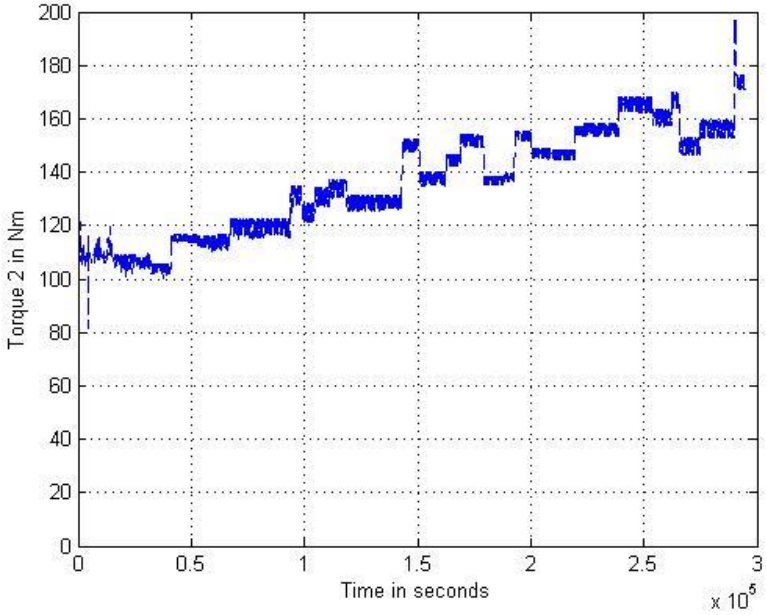


**Figure 5.10: Torque of motor 2**

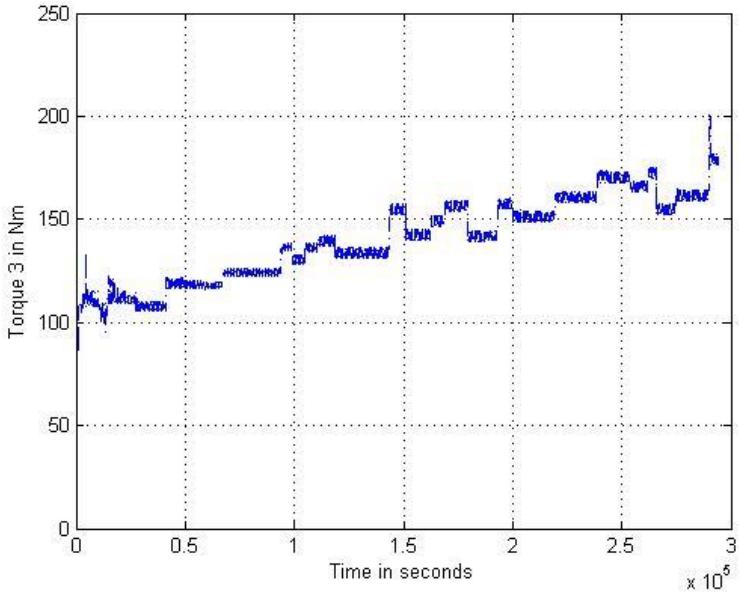


**Figure 5.11: Torque of motor 3**

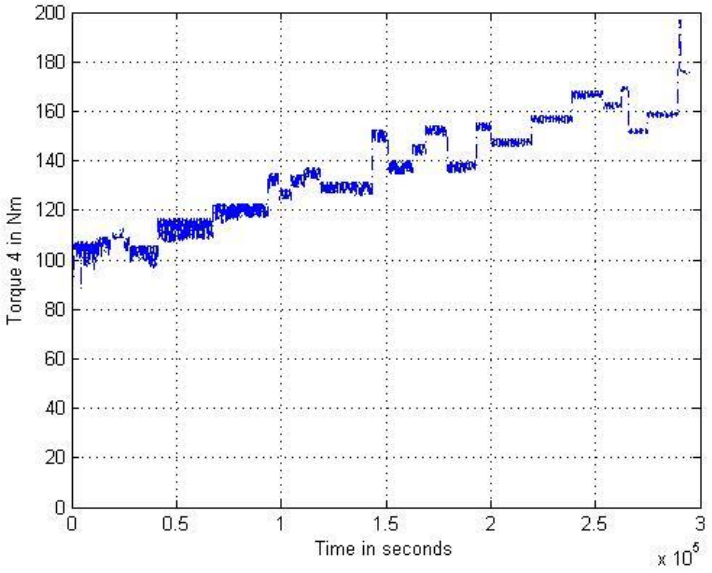


**Figure 5.12: Torque of motor 4**

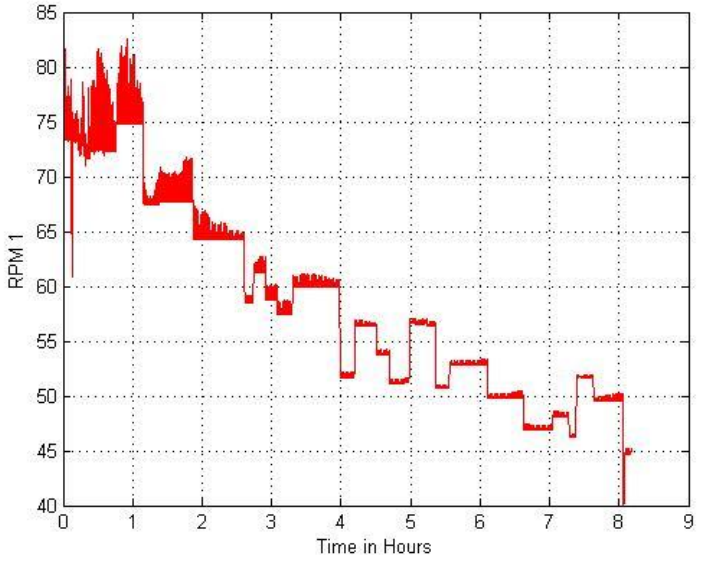


**Figure 5.13: RPM of motor 1**

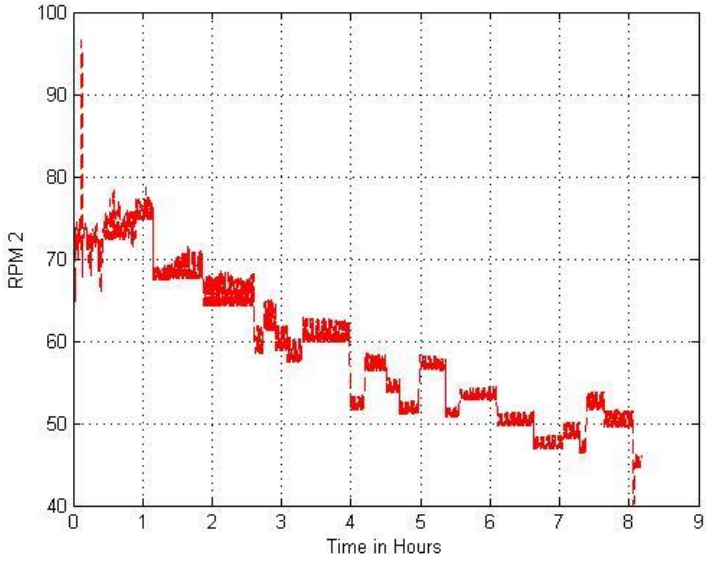


**Figure 5.14: RPM of motor 2**

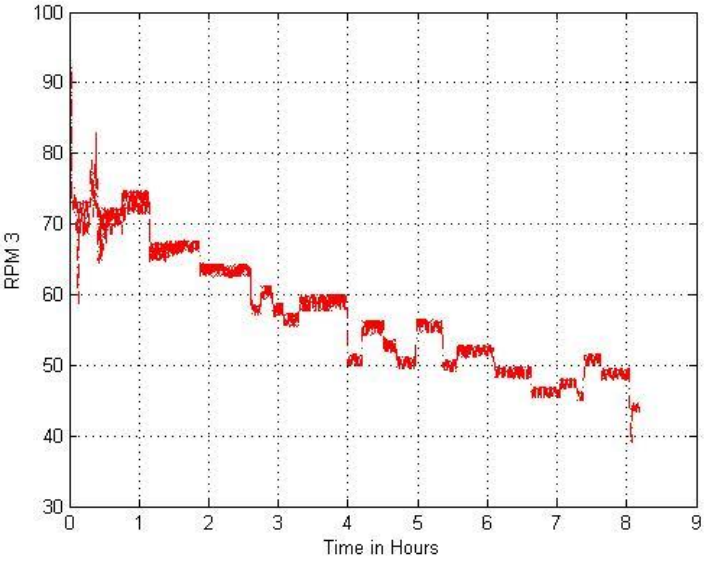


**Figure 5.15: RPM of motor 3**

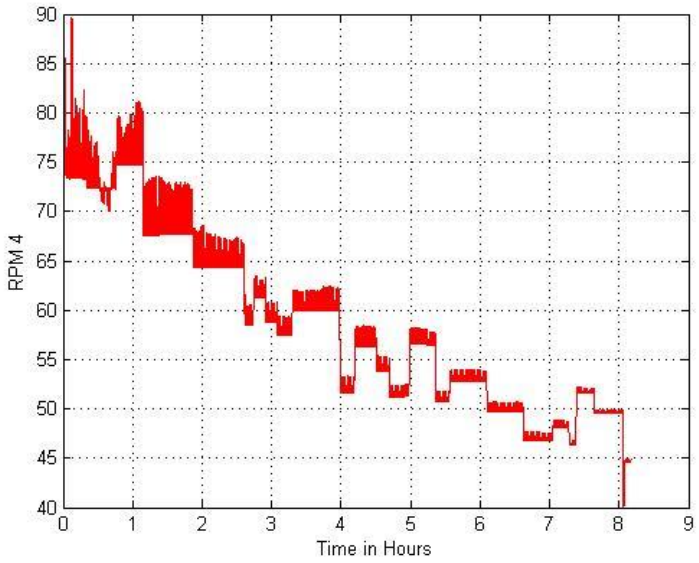


**Figure 5.16: RPM of motor 4**

### 5.4.1 Analysis of Results:

**Figure 5.4** is the reference trajectory which we are using for our simulations. From **Figure 5.5** and **Figure 5.8** it can be observed that the Liner estimated system follows the reference trajectory with a high accuracy. The control signals generated for the linearized system is given to the Non-Linear Model and a trajectory shown in **Figure 5.6** is obtained. On an error analysis of the results, it is observed that the difference in the target trajectory to the actual trajectory is greater than the Linear Model results but is still in an acceptable range (**Figure 5.7**). Also it can be observed that the control gradually adapts to the dynamics of the system and the error decreases with time. **Figure 5.9, Figure 5.10, Figure 5.11** and **Figure 5.12** shows the variation in torque and it can be observed that torque increases or decreases based on the increase or decrease of the rock specific energy. **Figure 5.13, Figure 5.14, Figure 5.15** and **Figure 5.16** shows the corresponding variation in the rpms of the motors.

# CHAPTER 6

# COMPARISION OF MPC AND IPO

## 6.1 Introduction

From Chapter 4, we can observe that interior point optimization (IPO) technique was applied to the system having 9 degree of freedom namely torque of 4 motors, rpm of four motors and weight on bit. This technique was mostly used for optimizing the rate of penetration of the system by varying the time factor during each step of simulation. In order to do a qualitative comparison between MPC and IPO, we reduced the degree of freedom factor to 4 namely the torques of the motor and simulated the system using IPO under the constrains mentioned in **Table 6.1**

**Table 6.1: Constrains for Simulations**

| Parameter | Value |
|---|---|
| **Torque 1** | 50-500 Nm |
| **Torque 2** | 50-500 Nm |
| **Torque 3** | 50-500 Nm |
| **Torque 4** | 50-500 Nm |
| **Time** | 60 sec |
| **RPM 1** | Function of Torque |
| **RPM 2** | Function of Torque |
| **RPM 3** | Function of Torque |
| **RPM 4** | Function of Torque |
| **WOB** | 500 N |

It is to be noted that these set of conditions are used only for the sake of comparison and the performance of the system obtained by them is not the definitive solution for determining

the best technique used for controlling the system as each technique has a unique principle of operation and has certain requirements for their effective execution.

## 6.2 Results

### 6.2.1 IPO

*a) With minimization of cost function containing the Error and Inputs*

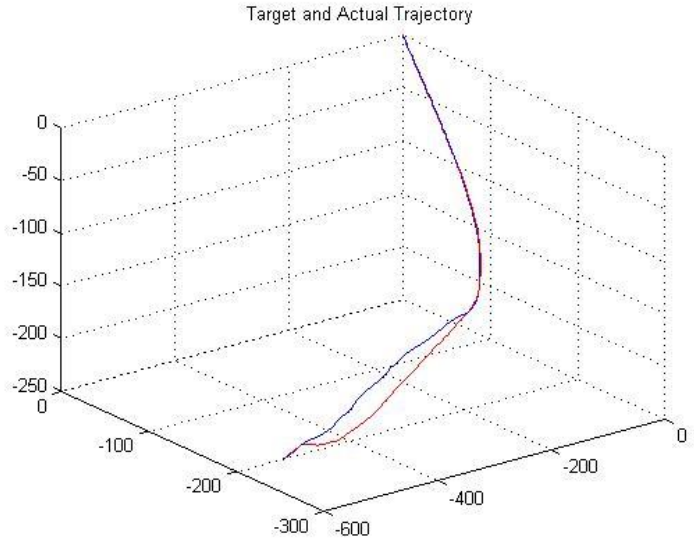


**Figure 6.1: Target and Actual Trajectory (IPO)**

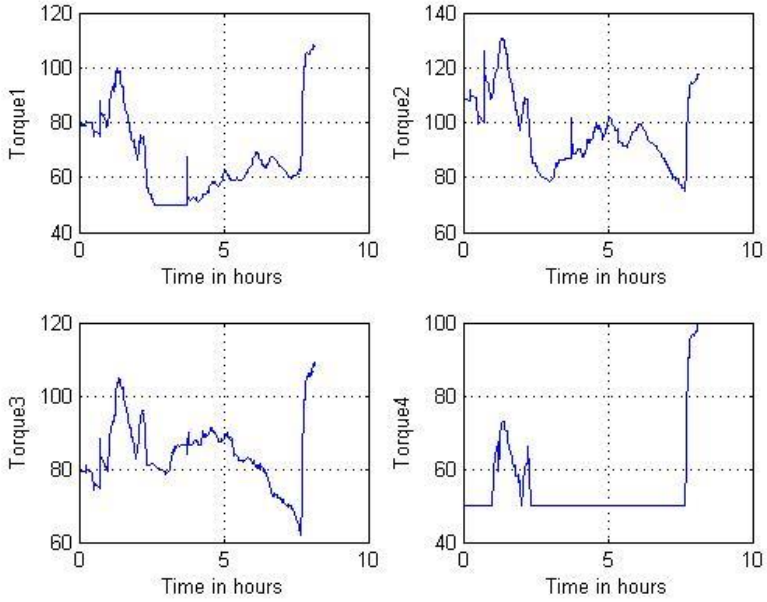


**Figure 6.2: Torques of the Motors (IPO)**

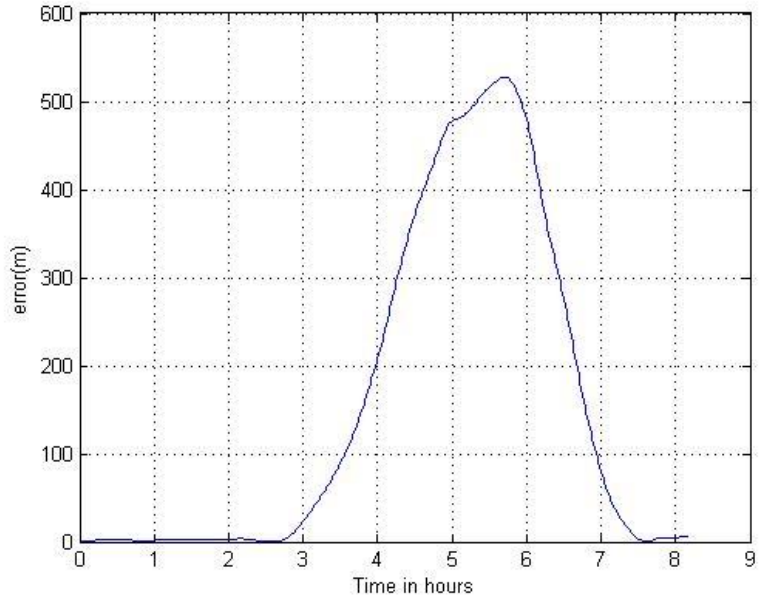


**Figure 6.3: Error in the Trajectory Tracking (IPO)**

*b) With minimization of cost function containing the Error only*

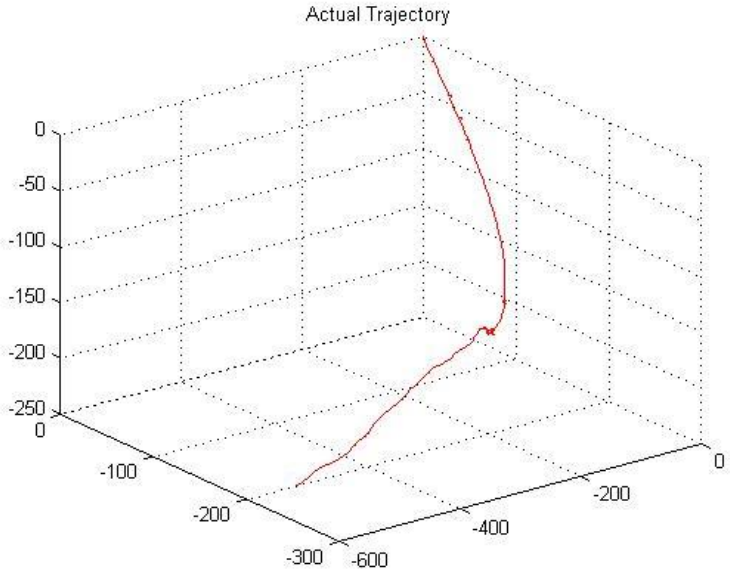


**Figure 6.4: Actual Trajectory of the System (IPO)**

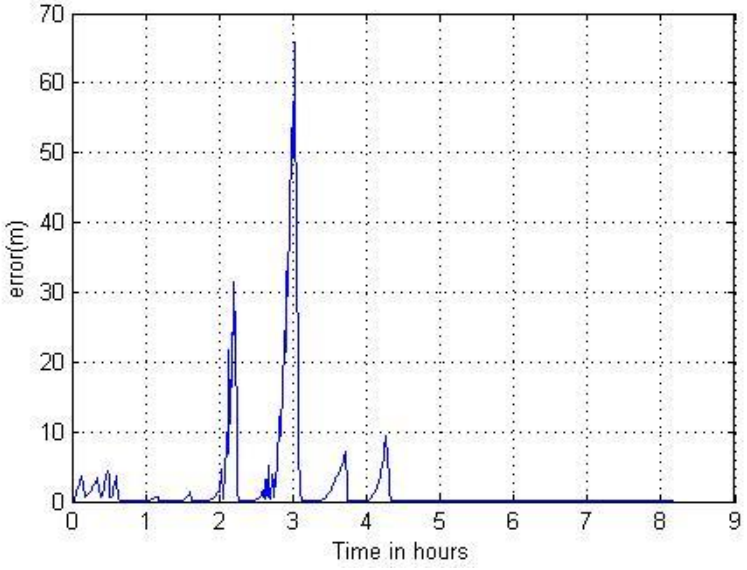


**Figure 6.5: Error in the trajectory (IPO)**

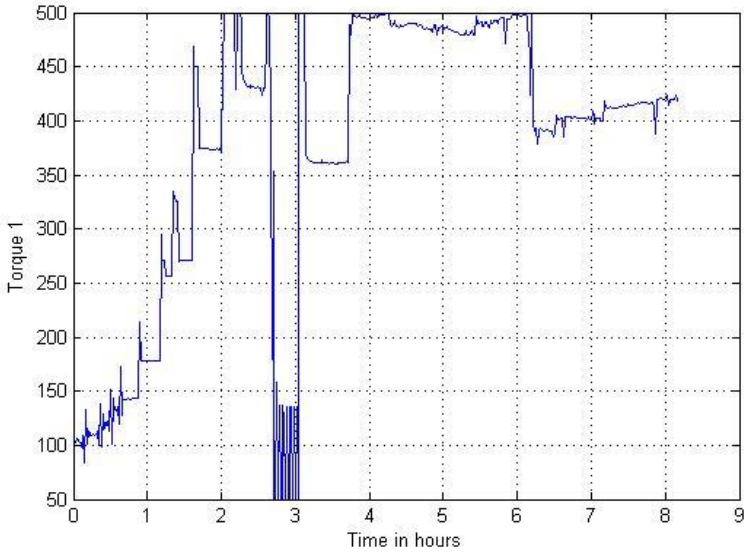


**Figure 6.6: Torque of motor 1 (IPO)**

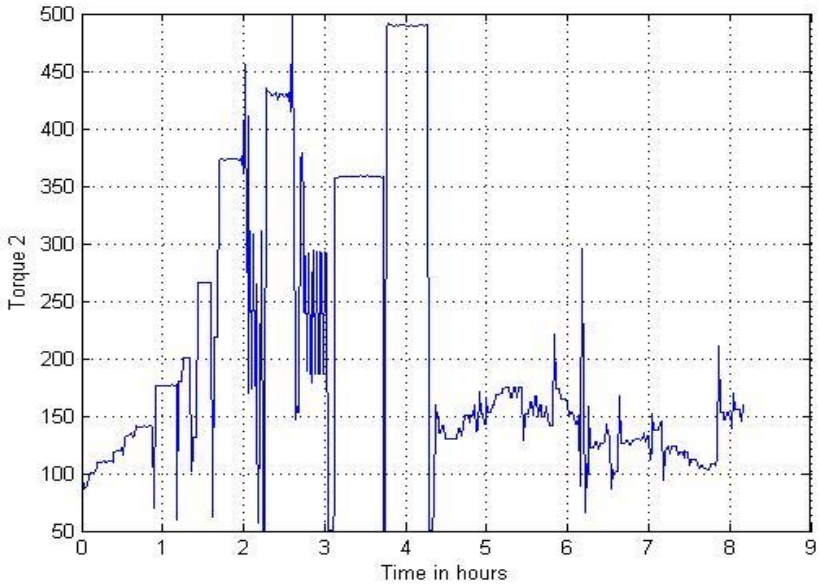


**Figure 6.7: Torque of motor 2 (IPO)**

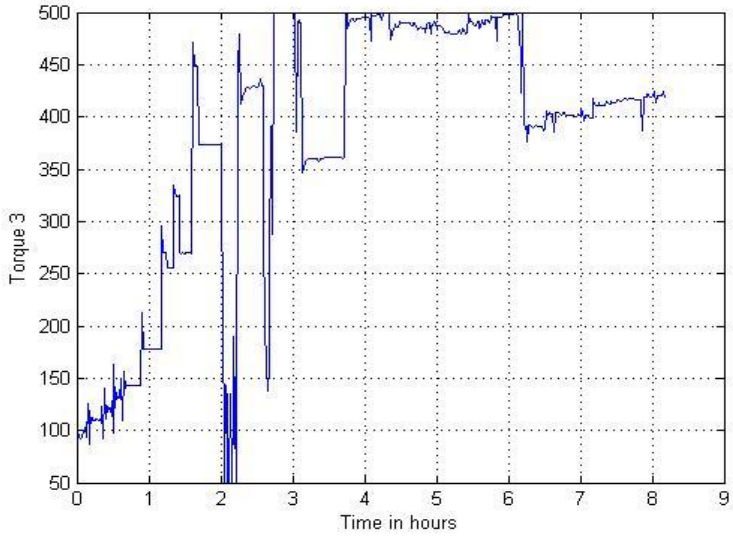


**Figure 6.8: Torque of motor 3 (IPO)**

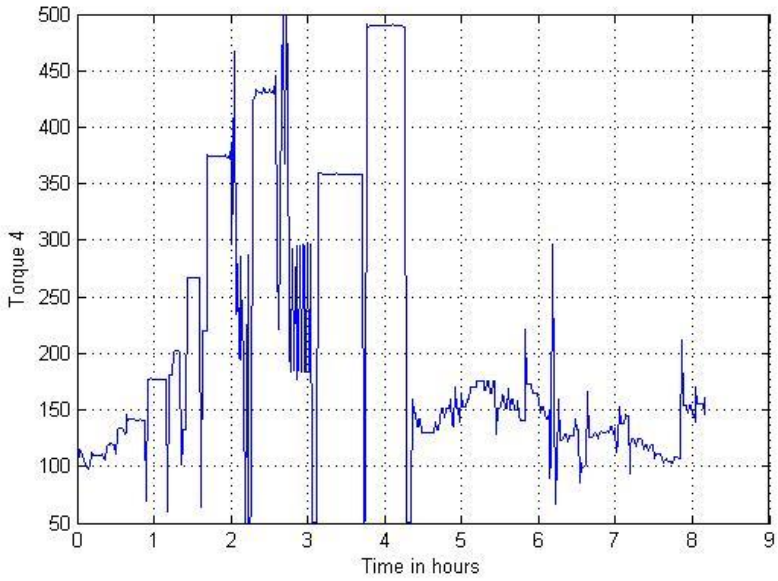


**Figure 6.9: Torque of motor 4 (IPO)**

## Analysis of Results (IPO):

**Figure 5.4** is the reference trajectory which we are using for our simulations. **Figure 6.1**is the target and reference trajectory for the first scenario optimizing error and inputs. **Figure 6.2** is

the error which is very high and exceeds the tolerance margin of 10 meters. **Figure 6.3** is the inputs for the simulation. Since the error is high, we will only consider the best case scenario for comparison and consider scenario 2 which is the cost optimization of error only. **Figure 6.4** shows the trajectory obtained by the system for scenario 2 using the IPO technique. It can be seen that there is a larger deviation from the path at some points and on doing an error analysis as shown in **Figure 6.5** we can observe that large deviations occur when there is a sizable change in the trajectory angle. **Figure 6.6** is the torque of the first motor, **Figure 6.7** is the torque of the second motor **Figure 6.8** is the torque of the third motor and **Figure 6.9** is the torque of the fourth motor. The torque graphs shows a sloppy control action generated by the IPO algorithm during the simulation.

### 6.2.2 MPC

The results obtained by the MPC simulations under the set of conditions from **Table 6.1** are as given in **Figure 5.5** to **Figure 5.12.**

### 6.2.3 MPC and IPO comparison

Error and input graphs of MPC and IPO techniques are merged to assist in comparison of the techniques and drawing conclusions.

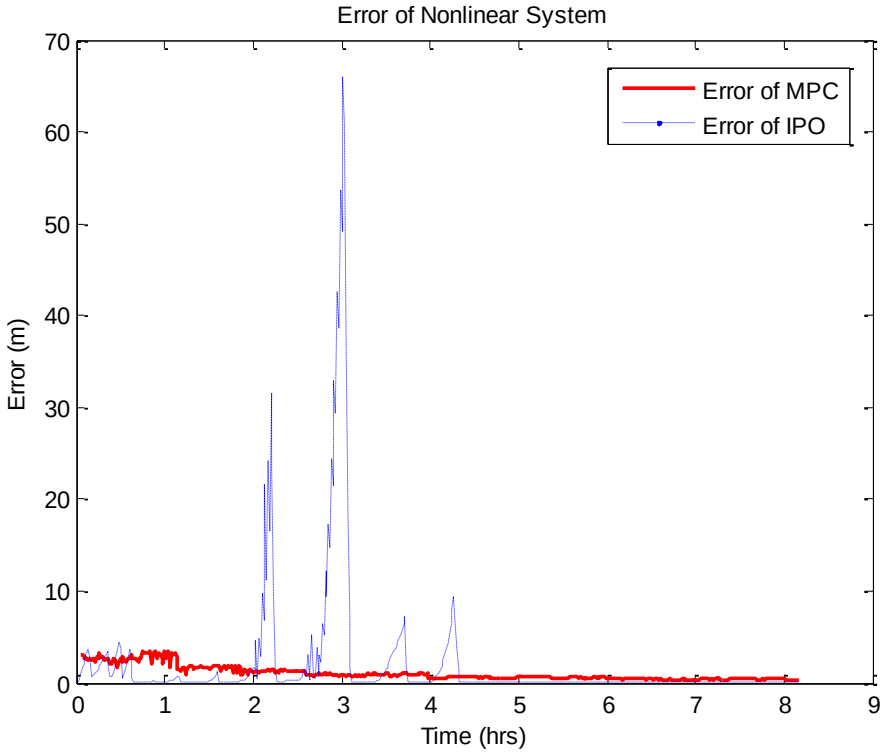


**Figure 6.10: Error plot (MPC/IPO)**

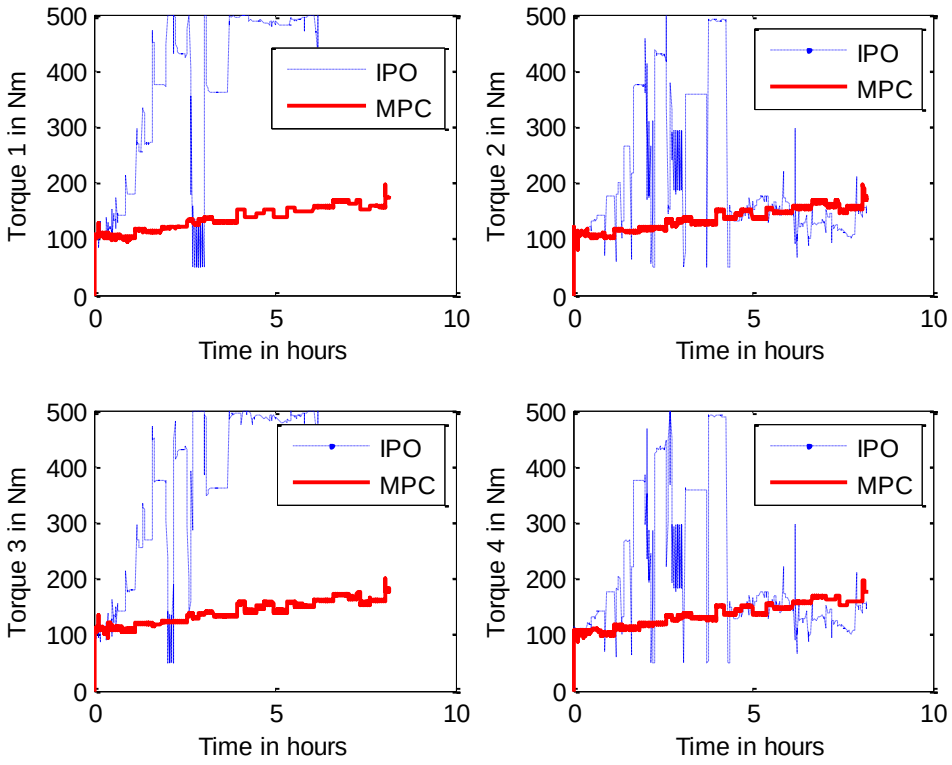


**Figure 6.11: Input Torques (MPC/IPO)**

## Analysis of Results (MPC/IPO):

**Figure 6.10** shows the combined error plot of the techniques. It can be observed that while the error gradually reduces in the system using an MPC, the IPO have a comparative rough response. For IPO, the errors occasionally shoots up along the trajectory and in 2 instances even crosses the tolerance level of 10 meters. A similar behavior can be observed in the system inputs of the IPO simulation, where in the inputs greatly fluctuates between the boundary conditions and there is no smooth transition in values as observed in the MPC technique **Figure 6.11.**

# CHAPTER 7

# CONCLUSION AND FUTURE WORK

## 7.1 Conclusion

From the Figure 6.10 and Figure 6.11, it can be observed that even though the IPO have a low average error in comparison to MPC, but under sudden change in the trajectory angles and less degree of freedom, the systems produces large errors as depicted by the spikes in the error graph. Also, for a trade off on the inputs to error margin (Figure 6.3) the error is very large and exceeds the tolerance range of 10 meters.

Under similar conditions, an IPO technique was applied to the system and results were studied. The system showed rugged response to the control algorithm and occasionally error in the path followed by the system exceeded the tolerance limit.

It can be concluded that if we have a higher DoF for control, a high level of tolerance for errors and need an optimization of ROP then IPO technique takes precedence as the control technique of choice. While, if the system lack in number of control inputs or we require a smooth mode of operation while optimization of ROP is not compulsory we can adopt MPC.

## 7.2 Future Extension

For future extensions on the project, it would be expressive to list them out as follows

1. **Complete utilization of DoF in the system**

As it can be observed, there is yet a potential for utilizing all the DoF existing in the system. For example, along with position, angles should considered for output so that the system will not only reach the desired position but will also be oriented in the correct angular direction.

Also adaptive control techniques could be investigated for its performance on this system. The drilling fluid dynamics could be considered in the system model to enhance the accuracy of the simulation with that of a prototype.

2. **Setup for Live Experiments**

   There is an immense potential for realizing this system as a live experiment. Collaboration with drill companies for enhancing, modifying and testing the prototype of the system is recommended.

3. **Use in the application Industry**

   On feed-back from the industrial experts, it was determined that the current Design is suitable for use in application industry for trench less laying of cables and pipes as the rocks are relatively soft and pressure is relatively low on the superficial surface of the earth crust than those around the oil wells. This will give a good insight on the behavior of the system on the fields.

.

# References


Aarrestad, T.V., SPE, And Blikra, H., SPE, Statoil A/S," Torque And Drag-Two Factors In Extended-Reach Drilling", SPE 1994

Altindag, A., "Correlation of specific energy with rock brittleness concepts on rock cutting", The Journal of The South African Institute of Mining and Metallurgy, 2003

Arnis Judzis and Ronald G. Bland," Optimization of Deep drilling Performance – Benchmark testing drives ROP improvements for bits and Drilling fluids", SPE 2009

Astrom, K.J., Bohlin, T., Numerical Identification of linear dynamic systems from normal operating records. IFAC Symposium on Self-Adaptive systems, Teddington, England (1965).

Baker, R. (2001). A primer of oil well drilling. 6th Ed., Publ. Petroleum Extension Service, Austin Texas.

Belaskle, J.P., SPE, Anadrili/Schlumberger, Dunn, M.D., SPE, Arco Alaska Inc, And Choo, D.K., SPE, Schlumberger," Distinct Applications Of MWD, Weight On Bit, And Torque", SPE 1993

Bemporad, M. Morari., N.L. Ricker, Model Predictive Control Toolbox: User Guide, The Math Works, Inc., Natick, 2012a.

Bourgoyne, A.T., Chenevert, M.E., Millheimand, K.K., Young, F.S., "Applied Drilling Engineering," Society of Petroleum Engineering (SPE), 1986.

Box, G.E.P., Jenkins D.R., Time-series analysis, Forecasting and Control. Holden-Day, San Francisco. (1970).

Cavanough. G.L., Member, IEEE, Mark Kochanek, Jock B. Cunningham, and Ian D. Gipps," A Self-Optimizing Control System for Hard Rock Percussive Drilling", 2008

Chen, Y., Lorentzen, R.J., and Vefring, E.H., "Optimization of well trajectory under uncertainty for Proactive Geosteering", SPE Journal, SPE-172497, 2015

Conti, P.F., "Controlled Horizontal Drilling," Society Of Petroleum Engineers International Association Of Drilling Contractors Drilling Conference, New Orleans, LA, USA, 1989.

Contreras, O., University of Calgary," An innovative approach for pore pressure prediction and drilling optimization in an Abnormally sub pressure basin", SPE 2012

Dahl, B. "Successful Drilling Of Oil And Gas By Optimal Drilling Fluid /Solid Control- A Practical And Theoretical Evaluation", SPE 2008

Downton, G.C., (2007), Directional Drilling System Response And Stability, Control Applications *CCA 2007.IEEE International Conference*, Pp.1543-1550, Singapore.

Eckerfield, R.J.," Data Gathering System For Drilling Optimization Work", 1997

ElShafei, M., Baig, M.M., Mysorewala, M.F., Majid, A.A., "Control and Optimization of Directional Drilling", SPE 716759, Middle East Intelligent Oil and Gas Conference, Abu Dhabi (2015)

Eustes, A.W., (2007)., "The Evolution of Automation in Drilling," SPE Annual Technical Conference, California, Nov. 2007. SPE 111125.

Favoreel, W., VanHuffel, S., DeMoor, B., Sima, V., Verhaegen, M., Comparative study between three subspace identification algorithms, Simulation, pp. 1-6. (1998).

Fear, M.J., SPE, Thorogood, J.L., SPE, Whelehan, O.P, SPE, and Williamson, H.S., "Optimization Of Rock·Bit Life Based On Bearing Failure Criteria", SPE 1992

Fisher, E. K. And French, M.R., "Drilling The First Horizontal Well In The Gulf Of Mexico: A Case History Of East Cameron Block 278 Well B-12," Society Of Petroleum Engineers Annual Technical Conference And Exhibition, Dallas, TX, USA, 1991.

Fisher, R.A., On an absolute criterion for fitting frequency curves. Mess. Math., 41:155. (1912)

Fu, J., Li, G., China University of Petroleum," A novel tool to improve the Rate of penetration-Hydraulic pulse Cavitating Jet generator", SPE 2012

Gong, M., and Liu, C.," Optimization for Multi-Objective Optimal Control Problem And Its Application In 3D Horizontal Wells", 2006

Graves, K.S., SPE, "Casing During Drilling with rotary Steerable Technology in the Stag Field", 2013

Haque, M.A., Chemical Engineering Department, "Locating Optimum Location For Well Drilling Using Genetic Algorithms",2002

Haugen, J., "Rotary steerable system replaces slide mode for directional drilling applications," Oil & Gas Journal, vol. 96, no. 9, pp. 65–71, 1998

Huerta, F., Cobreces, S., Rodriguez, F.J., Moranchel, M., Sanz, I., State-space black box model identification of a voltage-source converter with LCL filter, 3rd IEEE International Symposium on Power Electronics for Distributed Generation Systems. (2012).

Imrich, P., Institute Of Geotechnics Slovak Academy Of Sciences, Kosice, Slovakia," Fuzzy Knowledge Base In Evaluation Of Drilling", 1996

Joshi, S. D. and Ding W., (1991), "The Cost Benefits of Horizontal Drilling," American Gas Association, Arlington, VA, USA.

Karkoub, M.," Drill-String Torsional Vibration Suppression using GA optimized controllers", SPE 2009

Karu, E., "Hydraulic Optimization Of Foam Drilling For Maximum Drilling Rate In Vertical Wells", SPE 2005

Katayama, T., Subspace Methods for System Identification. London: Springer-Verlag. (2005).

Koederitz W.L., and Johnson, W.E., “Real-Time Optimization of Drilling Parameters by Autonomous Empirical Methods”, SPE/IADC Drilling Conference and Exhibition, SPE-139849-MS, 2011

Latha, B. and Senthilkumar, V.S. ” Simulation Optimization of Process Parameters in composite drilling process Using Multi objective Evolutionary Algorithm”, IEEE 2009

Ljung, L., System Identification Toolbox: User Guide, Math Works, Inc., Natick, 2012b.

Maciejowski, J.M., "Predictive control with constraints," Upper Saddle River, Nl: Prentice-Hall, 2002.

Marck, J., and Detournay, E “Influence of Rotary–Steerable-System Design on Bore hole Spiraling”, SPE Journal, SPE-174554, 2015

Meng, C., and Ying-hu, Z., “Applied Research of Scheme Optimization in the Drilling Support System ”, IEEE 2010

Motahhari, H.R., hareland, G., Nygaard, R.,” Method of Optimizing Motor and Bit Performance for Maximum ROP”, SPE 2009

Onwunalu, J.E., SPE, “A new well pattern optimization procedure for large scale field development”, SPE 2011

Osterloh W.T., And Menard, W.P., “New Method Combines Simulation And Novel Spreadsheet Tools To Enable Direct Optimization Of Expansion Decisions In A Giant Heavy Oil Filed”, SPE 2007

Overschee., P.V., Moor, B.D., N4SID: Subspace Algorithms for the Identification of Combined Deterministic-Stochastic Systems, Automatica, Vol. 30, pp.75-93. (1994).

Panchal, N., Bayliss, M.T., Whidborne, J.F., “Attitude control system for directional drilling

Park, B., Kim, J., Park, J., Shin, J. and Myung, H., “Hybrid 4-Pad Rotary Steerable System for Directional Drilling of Unconventional Resources”, 2013

Pecht E., And Mintchev, M. P., Senior Member, IEEE,” Modeling Of Observability During In-Drilling Alignment For Horizontal Directional Drilling”, 2007

Rashidi, B., Hareland, G. and Nygaard.R, “Real-Time Drill Bit Wear Prediction by Combining Rock Energy and Drilling Strength Concepts,” Abu Dhabi international Petroleum Exhibition and Conference, 2008, SPE-117109.

Skalle, P., Norwegian University of Science and Technology,” Detection of Symptoms for Revealing Causes Leading to Drilling Failure”, SPE 2013

Spanos, P.D., Sengupta, A.K., Cunningham, R.A., and Paslay, P.R. “Modeling of roller cone bit lift-off dynamics in rotary drilling,” Journal of Energy Resources Technology, 117(3):197–207, 1995.

Sui, D., and Nybø R., and Azizi, V., “Real-time Optimization of Rate of Penetration during Drilling Operation”,

Talib, M., Elshafei, M., Khoukhi, A., Saif, A.W., Abdulaziz, A., "Modeling And Control Of Quad-Motor Directional Steering System", Proceedings Of The Ieee SYMPOSIUM ON Innovations In Intelligent System And Applications (INISTA) , June, 2014.

Tucker, R.W., and Wang, C., "An integrated model for drill string dynamics," Journal of Sound and Vibration 224(1), 123-165, 1999.

Tuna, Evren, M. Ozbayoglu," Real Time Optimization of Drilling Parameters during Drilling Operations", SPE Oil and Gas Conference and Exhibition, Mumbai, 20-22 January 2010.

Warren, T., Houtchens B., and Madell, G. "Directional Drilling with Casing", SPE Drilling and Completion, SPE-79914, 2005

# Vitae

| | |
|---|---|
| Name | :Mirza Mohibulla Baig |
| Nationality | :Indian |
| Date of Birth | :8/4/1989 |
| Email | :mmbaig.se@gmail.com |
| Address | :Arbayeen Street, Azizia District, Jeddah, Saudi Arabia |
| Academic Background | : 1) Bachelor of Engineering (B.S), Electronic and Instrumentation Engineering, Osmania University (2007-2011)<br>2) High School and Junior College, International Indian School (2003-2007) |
| Publication | : Moustafa ElShafei, **Mirza M. Baig**, Mohammed Mysorewala, Abdul Aziz Al Majid, "Control and Optimization of Directional Drilling", SPE 176759, Middle East Intelligent Oil and Gas Conference, Abu Dhabi (2015) |
| Experience | : **1) Automation Engineer (1 Year)**<br>**Al Mayssan Technical Services (MTS),**<br>For 2 projects using Schneider Quantum PLCs: BMS Control Panel Designing- Programming- Installation-Testing and Commissioning |

**2) Researcher cum Lab Instructor (2 Years)**

**King Fahd University of Petroleum and Minerals**

**For PLC Lab, Mechatronics Lab and Power Electronics Lab:** Guide students in various experiments- Update work progress- Conduct tests and allocate grades

**For Research:** Worked in the area of Directional Drilling, Proposed new Drill technology and Studied techniques in optimizing it.

Achievements : **1) University Gold Medal**

**Osmania University,**

Awarded a Gold medal for securing the first position in the EIE department of the Osmania University

**2) Scholarship by the University**

**King Fahd University of Petroleum and Minerals**

Awarded full scholarship to pursue Masters in Control engineering by the KFUPM.